Low Dimensional Magnetism Workshop

European School on Magnetism
Timisoara, Sept. 08, 2009

Pietro Gambardella
ICREA and Centre d'Investigació en Nanociència i Nanotecnologia (ICN-CSIC), Barcelona, Spain

Olivier Fruchart
Institut Néel (CNRS), Grenoble, France

Wulf Wulfhekel
Physikalisches Institut, Universität Karlsruhe, Karlsruhe, Germany

2 a

Magnetic moments: atoms vs. bulk

$$H = \sum_{i=1}^{Z} \frac{p_i^2}{2m} - \sum_{i=1}^{Z} \frac{Ze^2}{r_i^2} + \sum_{i<j} \frac{e^2}{|r_i - r_j|^2} + \sum_{i=1}^{Z} (\mathbf{l}_i \cdot \mathbf{s}_i) g(r_i) = H_C + V_{e-e} + V_{s.o.}$$

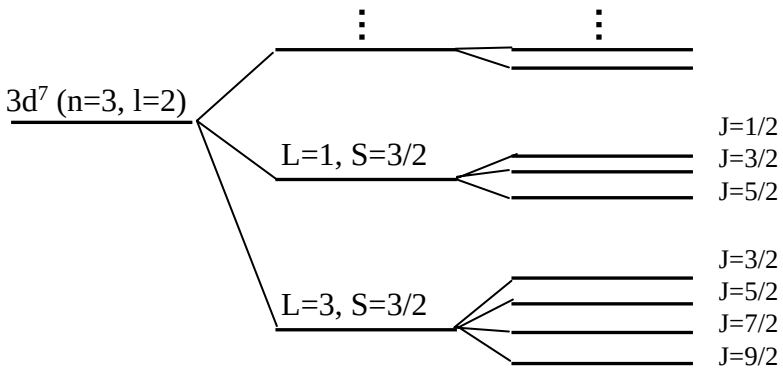

central field approximation

TERMS
electrostatic interaction
$|LSM_LM_S\rangle$ base

MULTIPLETS
spin-orbit coupling
$|LSJM\rangle$ base

Hund's rules:

1) Total spin $S = S_i s_i$ is maximized

2) Total orbital moment $L = S_i l_i$ is maximized

3) *L* and *S* couple parallel ($J=|L+S|$) if el. shell is more than half-filled,
L and S couple antiparallel ($J=|L-S|$) if el. shell is less than half-filled

see lecture 2 by J.M.D. Coey

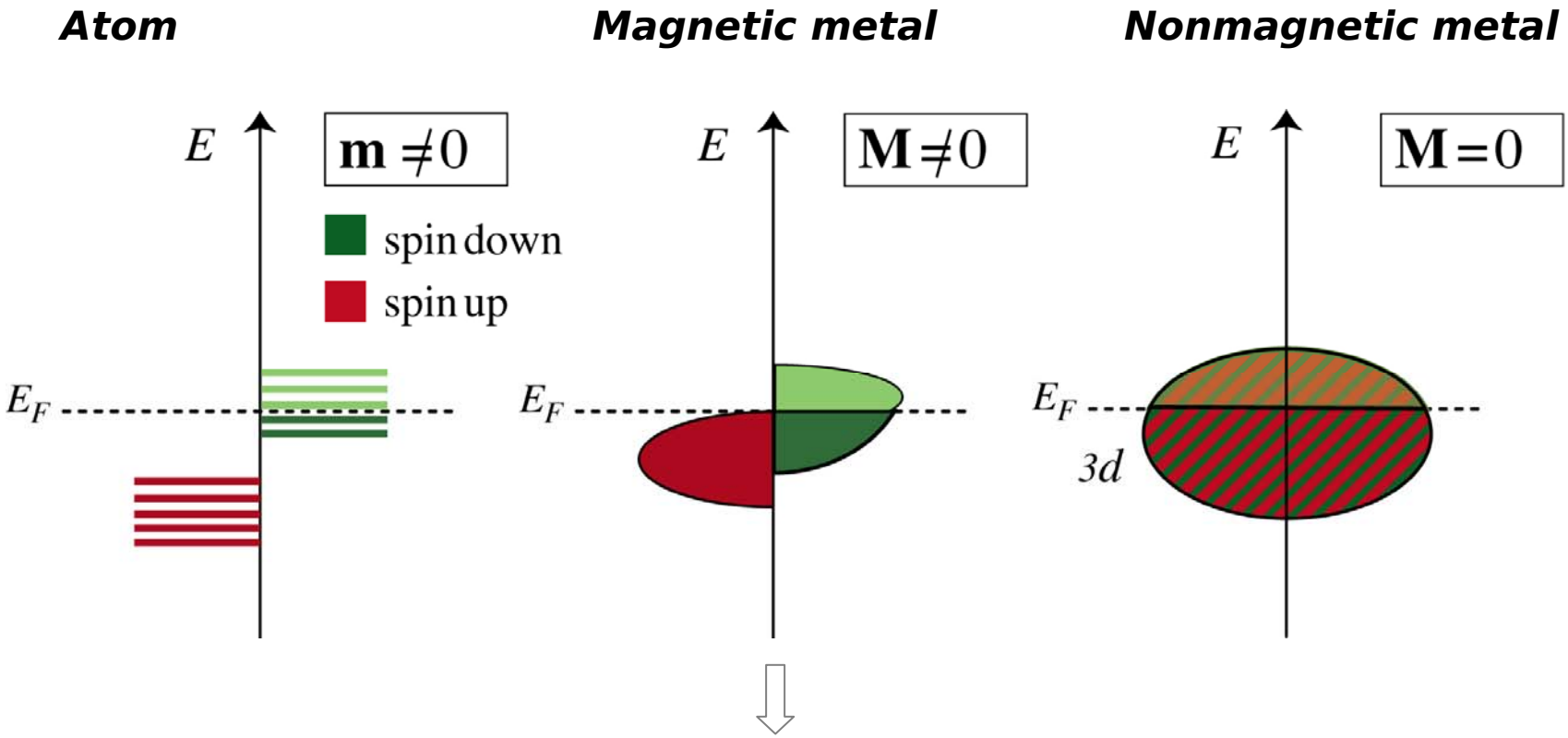

Material	N holes
Fe	3.4
Co	2.5
Ni	1.5

m_s^{tot}	m_s^{d}	m_s^{sp}
2.19	2.26	-0.07
1.57	1.64	-0.07
0.62	0.64	-0.02

m_{orb}
0.09
0.14
0.07

Data from O. Eriksson et al., Phys. Rev. B 42, 2707 (1990).

Free atoms vs. bulk: spin moment in 3*d* metals

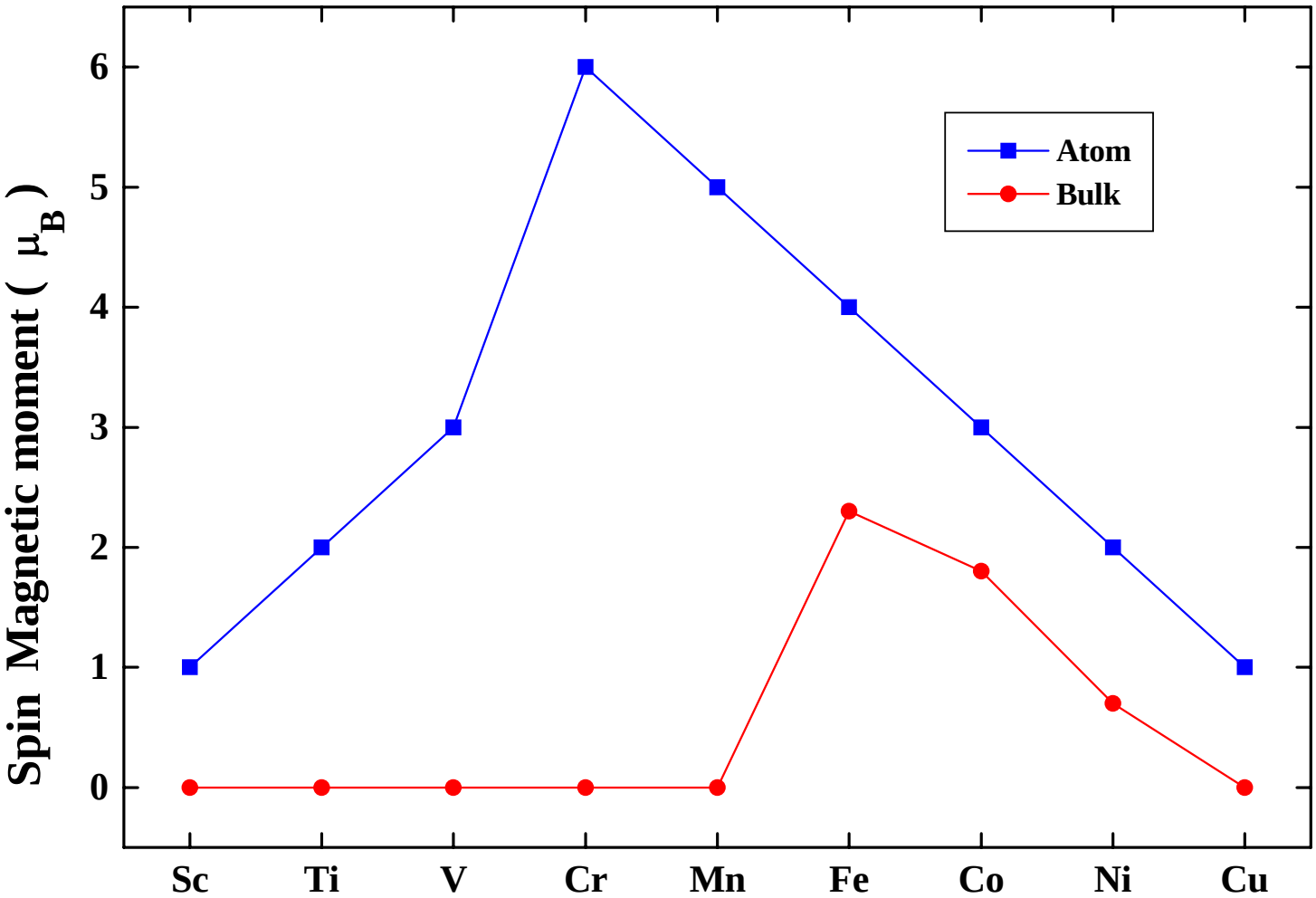

courtesy V. S. Stepanyuk, MPI Halle

Exchange-split electron band structure measured by UV photoemission

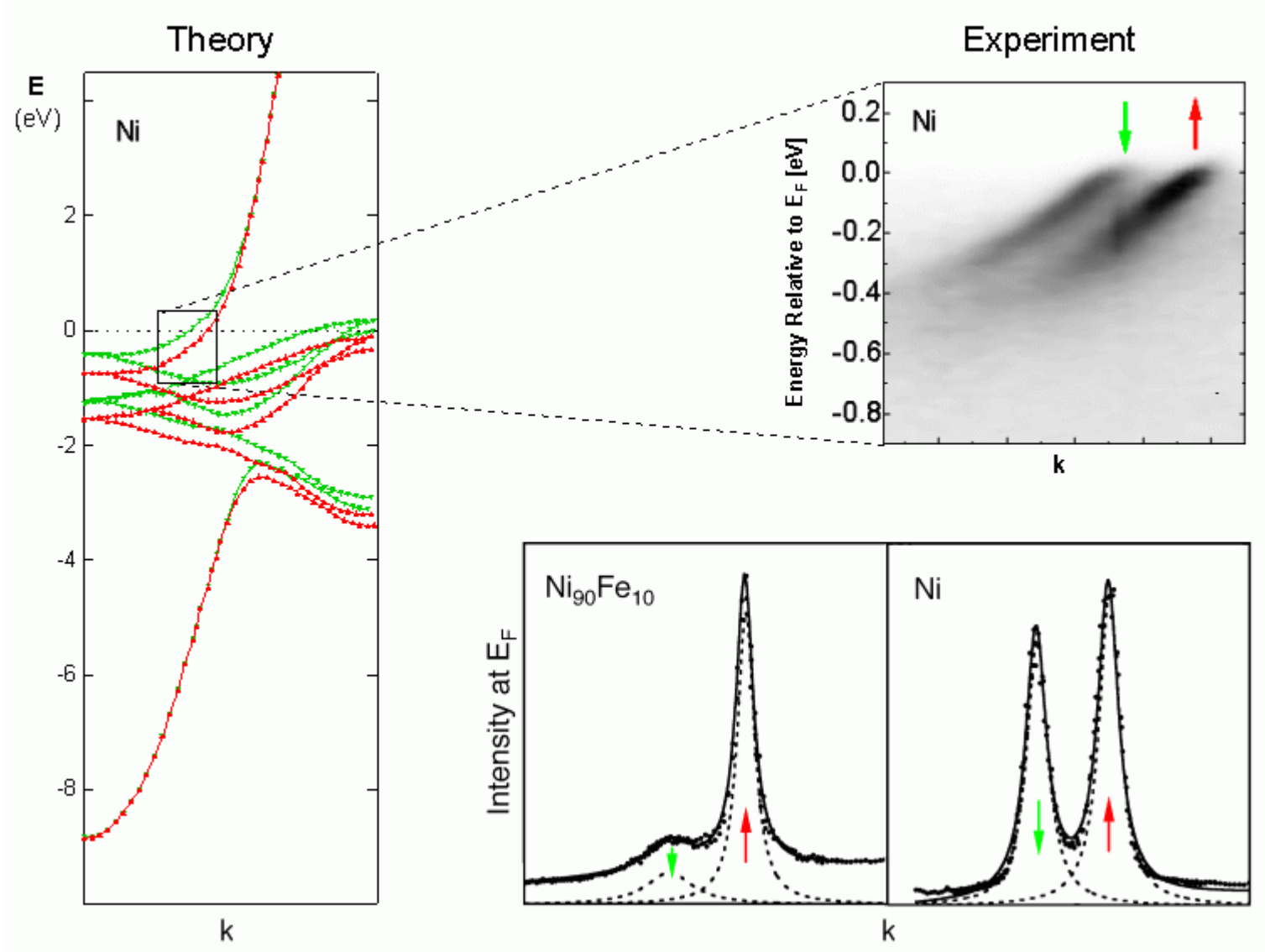

Himpsel et al., J. Magn. Magn. Mat. **200**, 456 (1999).

Exchange splitting vs. spin magnetic moment

Magnetic moment ~ exchange-splitting

$$\frac{\mu}{\Delta_{exc}} \approx 1 \frac{\mu_B}{eV}$$

Exchange-split density of states

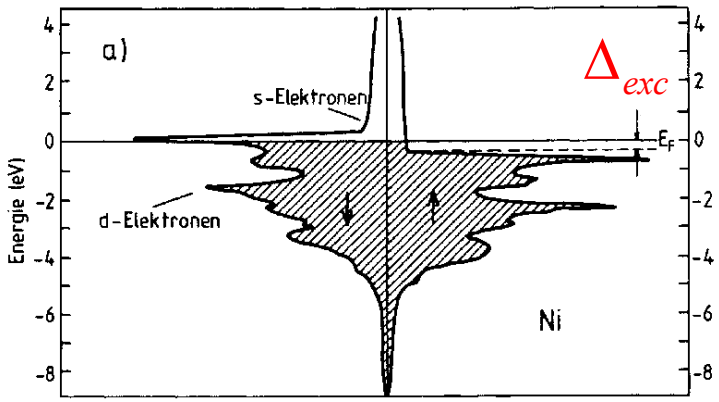

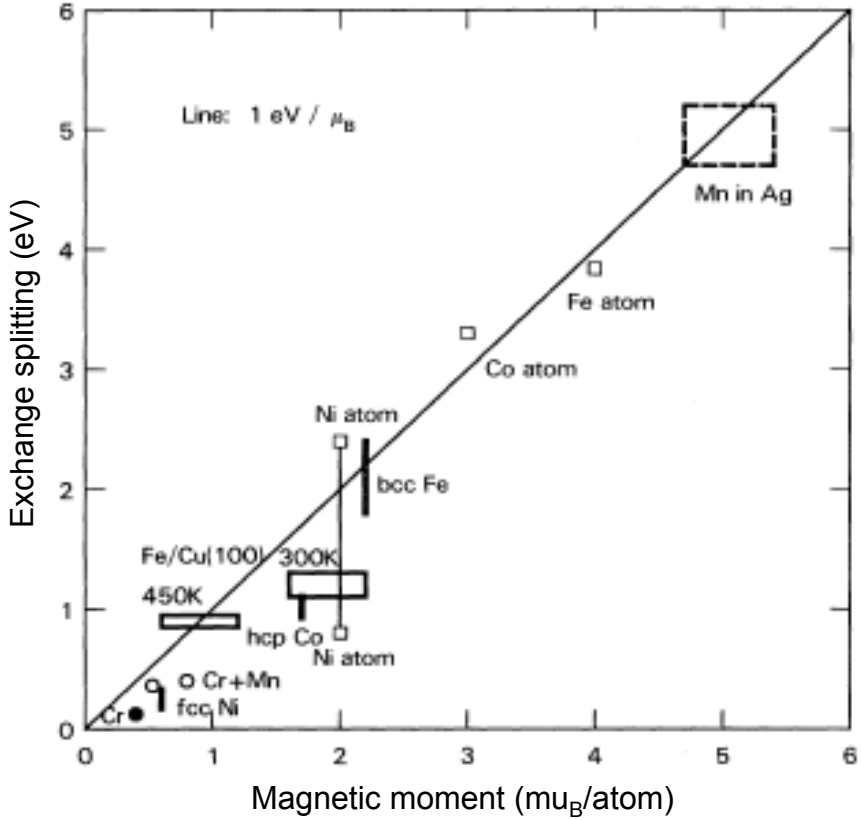

Himpsel, Phys. Rev. Lett. 67, 2363 (1991)

Stern-Gerlach experiment

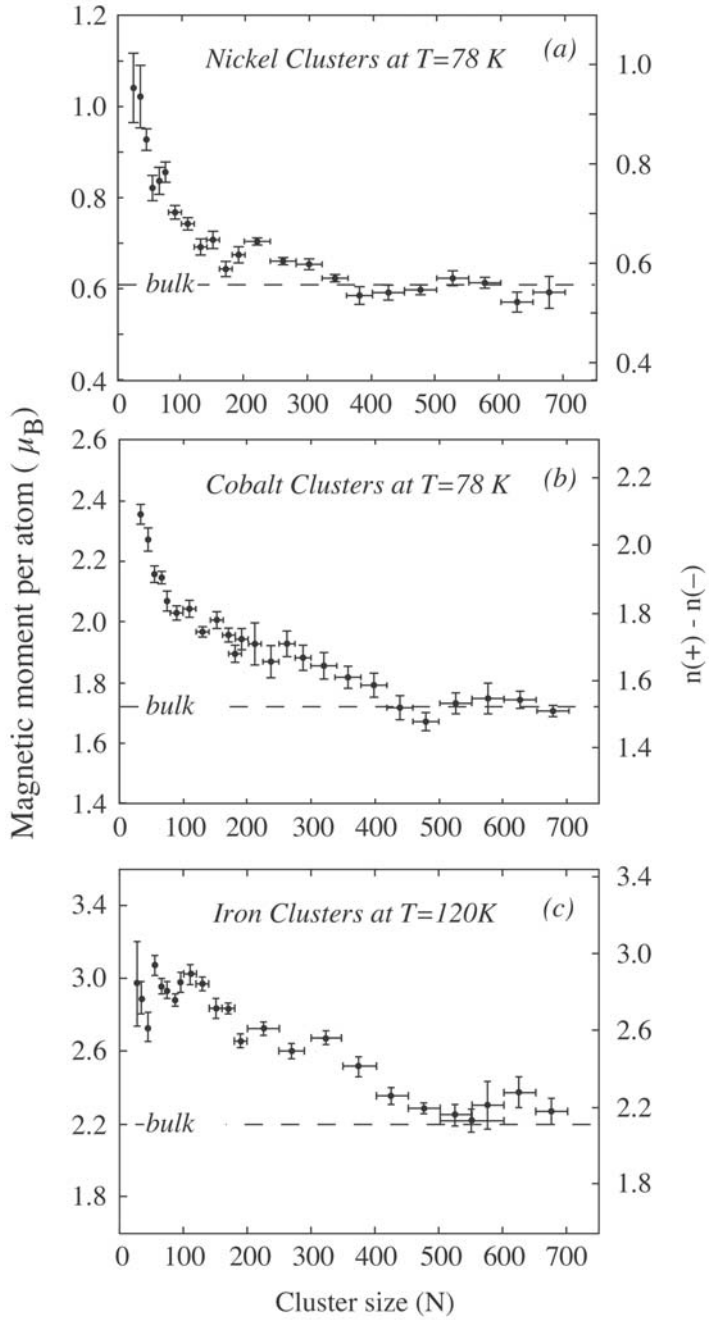

I.M.L. Billas, A. Châtelain, W.A. de Heer, Science 265, 1682 (1994).

bulk Fe DOS

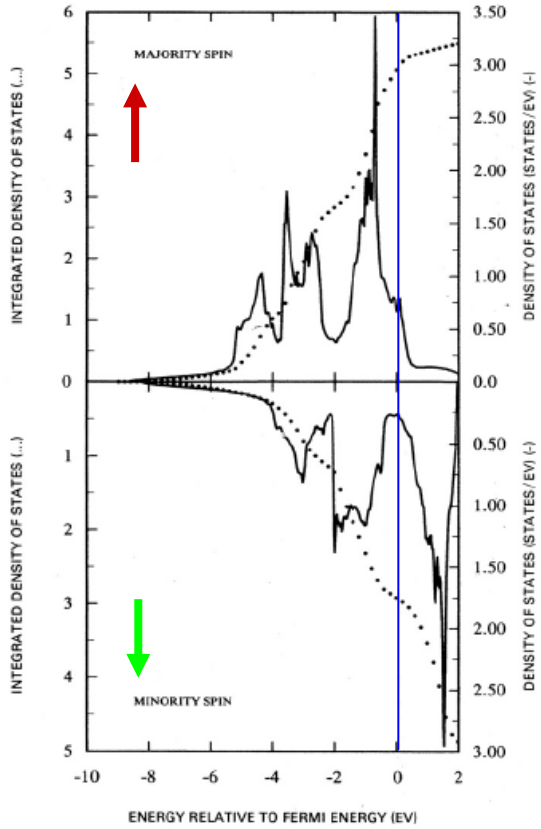

Moruzzi, Janak, and Williams,
Calculated electronic properties of metals
(Pergamon, 1978)

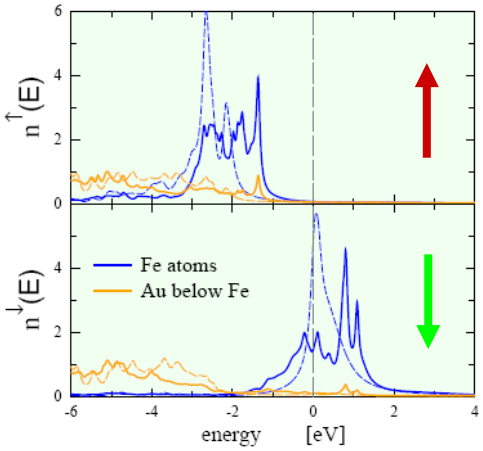

1 ML Fe/Au(111)

Fe_1/Au(111)

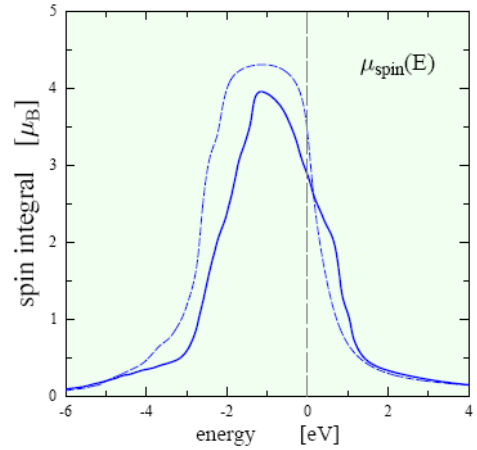

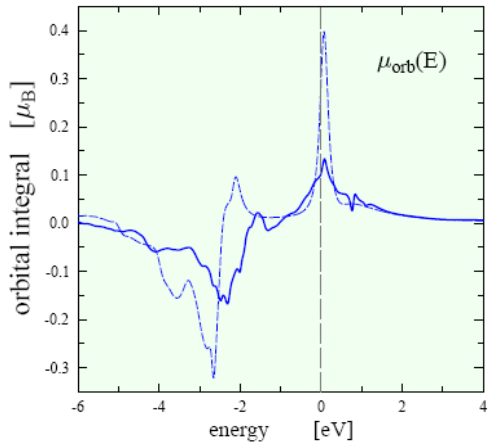

Sipr, Minar, and Ebert,
Europhys. Lett., in press (2009)

Enhanced magnetic moment at surfaces and 2D layers

Fe (100) and (110) surfaces

Symmetry-dependent increase in topmost layer magnetization

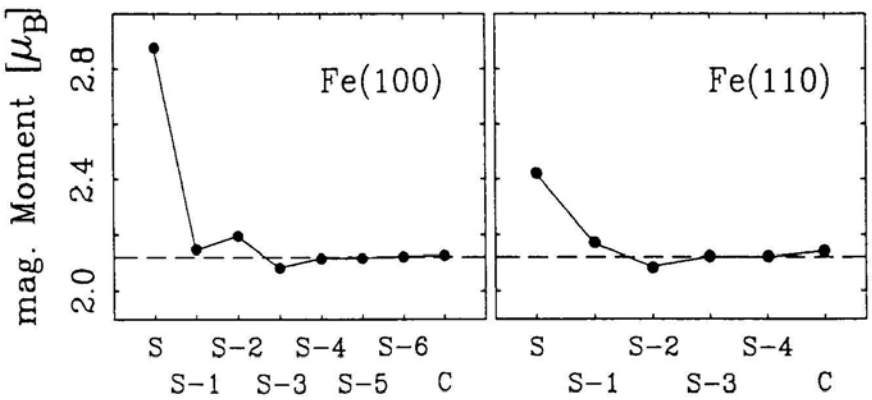

S. Handschuh, PhD thesis, Uni Köln

1 ML Fe on W(110):

15 % increase in ground state (T=0) magnetic moment

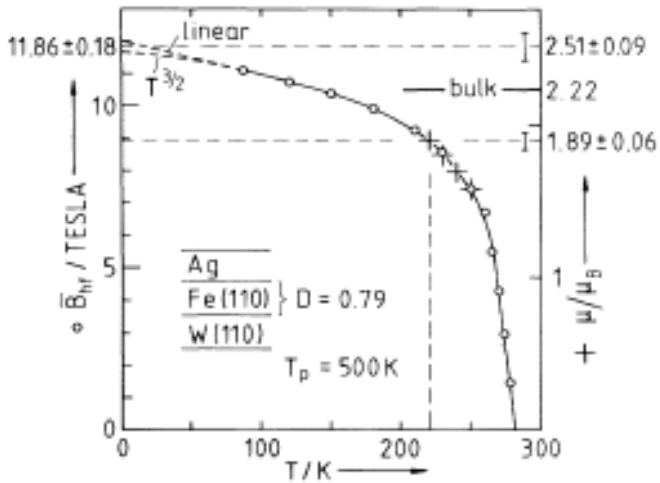

FIG. 4. Magnetic moment per atom in the remanent state, in units of Bohr magnetons, μ/μ_B (+), vs T for the monolayer film of Figs. 1–3 in comparison with the mean hyperfine field B_{hf} (○) of a film W(110)/0.82/Ag, determined by CEMS. $B_{hf}(0) = 11.86 \pm 0.18$ T is taken as the mean value between a $T^{3/2}$ and a linear extrapolation. B_{hf} and μ/μ_B are normalized at $T = 220$ K.

Elmers, Liu, and Gradmann, Phys. Rev. Lett. 1989

Coordination-dependent spin magnetic moment in metal clusters

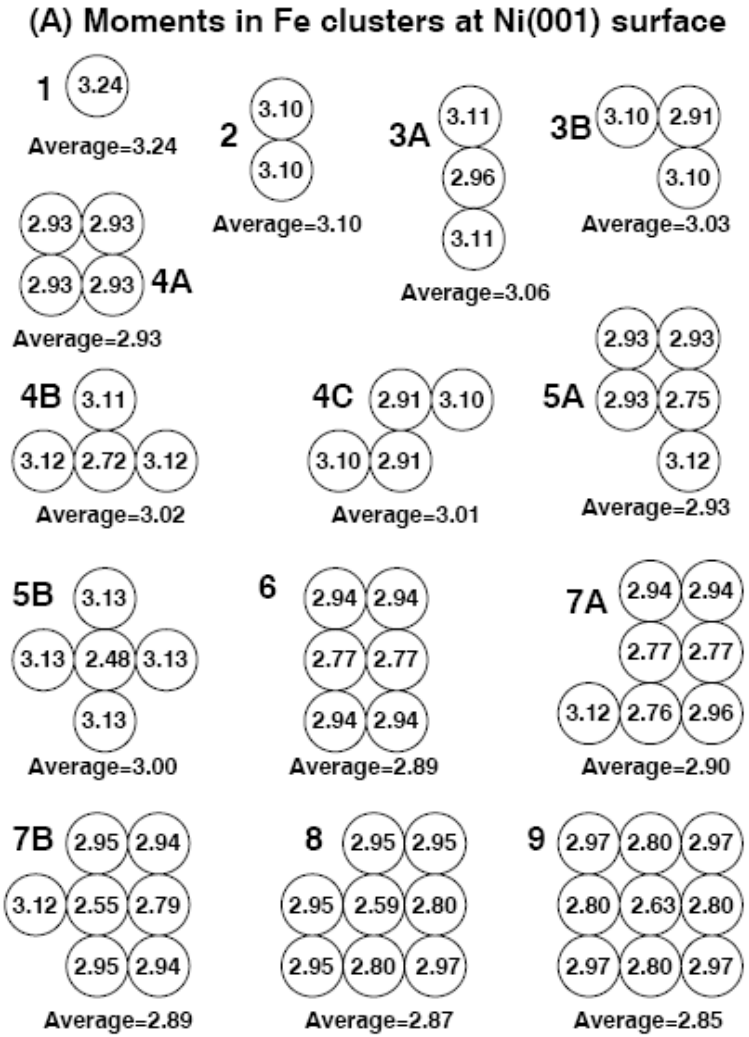

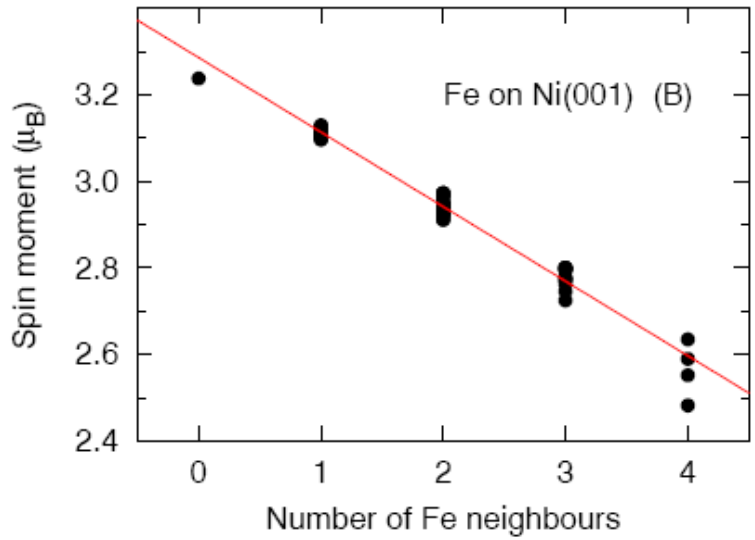

SP-KKR calculations, Mavropoulos, Lounis, Zeller, and Blügel, Appl. Phys. A 2006

Stoner criterion $U\, n(E_F) > 1$

Rectangular-shaped DOS

$$\int_W n(\varepsilon)\, d\varepsilon = const. \quad \Rightarrow n(E_F) \sim \frac{1}{W}$$

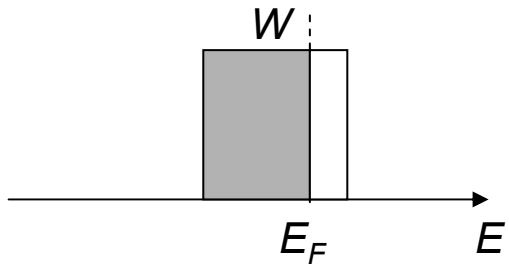

In transition metals:

$$n(E_F) \approx n_d(E_F) \sim \frac{1}{W_d}$$

Tight-binding:

$$W_d \approx 2\sqrt{N_{nn}}\, h_d(r_{nn})$$

nearest neighbors | hopping | lattice spacing

$$W_d^{\mathrm{ML}} : W_d^{(001)} : W_d^{\mathrm{fcc}} = 0.58 : 0.82 : 1$$

$$n_d^{\mathrm{ML}} : n_d^{(001)} : n_d^{\mathrm{fcc}} = 1.73 : 1.22 : 1$$

S. Blügel, FZ Jülich

2b 4d, 5d magnetism

$$I_{3d} > I_{4d} > I_{5d}$$

$$h_{3d} < h_{4d} < h_{5d} \Longrightarrow W_{3d} < W_{4d} < W_{5d} \Longrightarrow n_{3d} > n_{4d} > n_{5d}$$

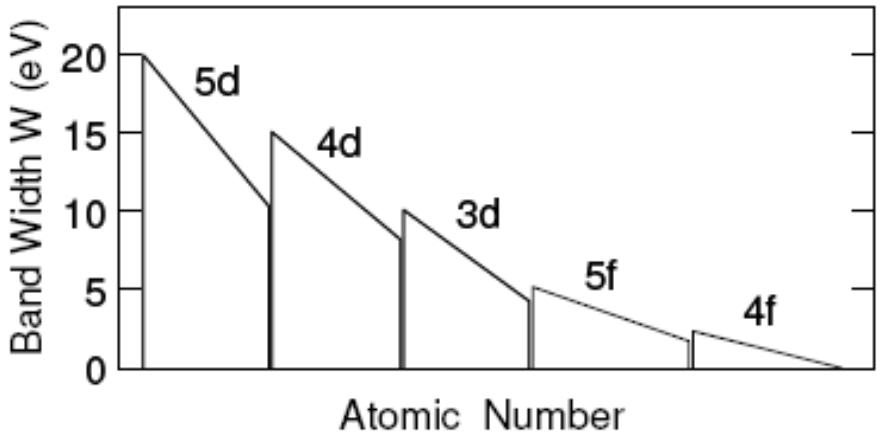

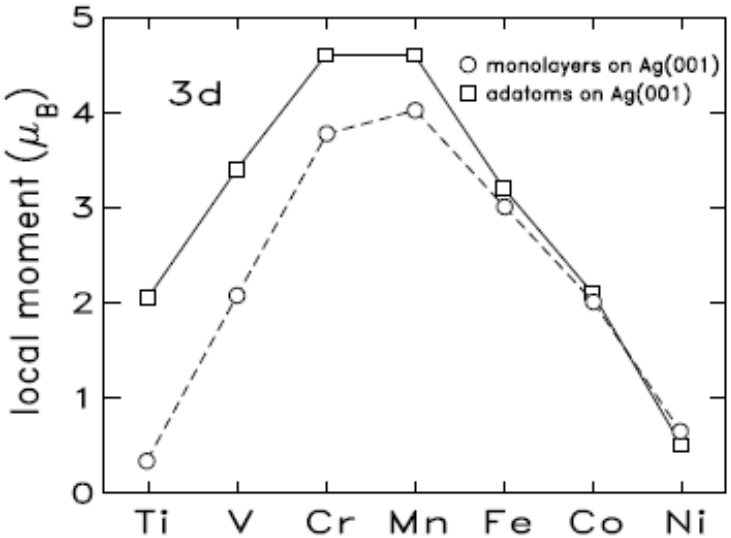

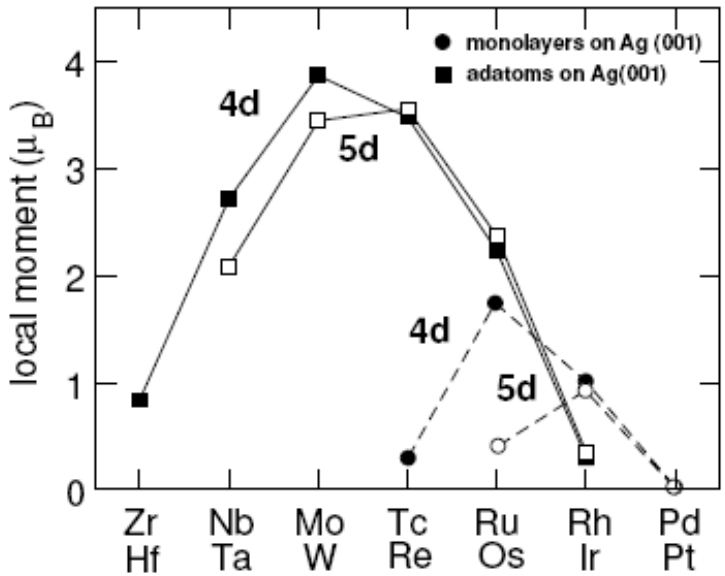

S. Blügel and P. Dederichs, FZ Jülich – Phys. Rev. Lett. 1992, Solid State Comm. 1994.

Nonzero magnetic moments in 4*d* metal clusters

Free clusters

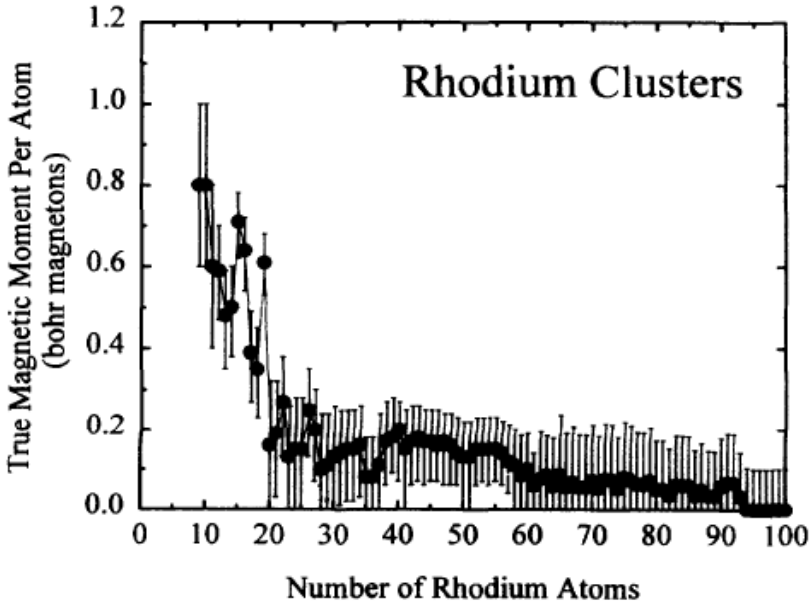

(superpara)magnetic if < 100 atoms

Cox et al., PRB 1994

Adatoms, adclusters

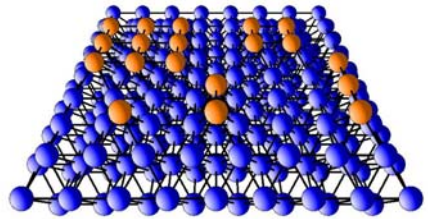

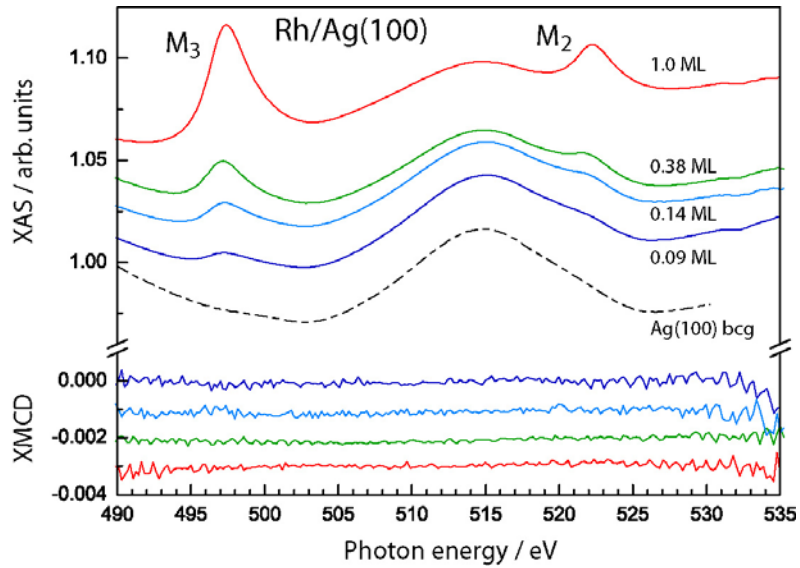

nonmagnetic

Honolka et al.,
Phys. Rev. B **76**, 144412 (2007).

Increase in total magnetization due to Pd deposition on a Fe film

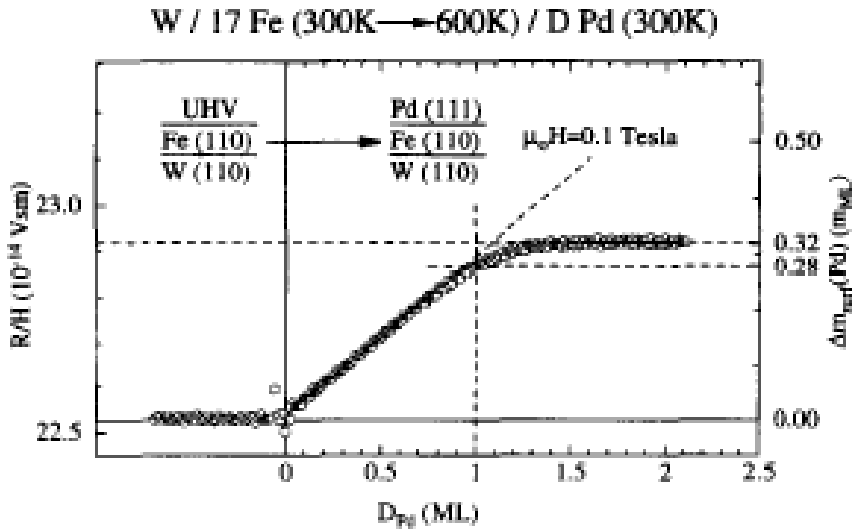

Fig. 1. TOM during coverage of 17 atomic layers of Fe(110) on W(110) by Pd. Fe film prepared at elevated temperatures, hence with a smooth surface. R/H (see Eq. (10)) measured versus number of Pd layers D_{Pd}. Measurements were performed at 300 K in a field of 0.1 T. R/H approximately equals the excess moment $\Delta\mu_{surf}(Pd)$, which is given in units of Fe monolayer moment m_{ML}.

Gradmann, Dürkop, and Elmers, JMMM 165, 56 (1997).

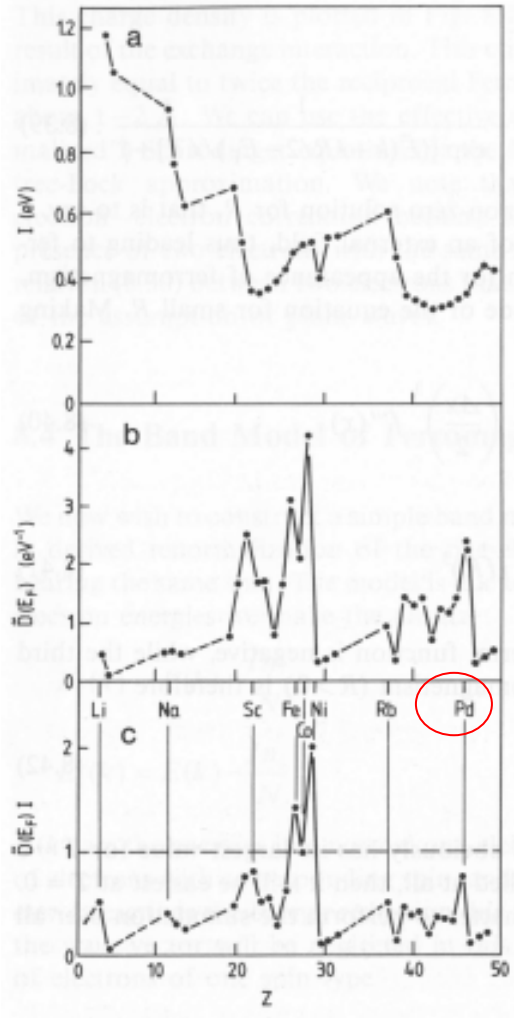

Janak, PRB 16, 255 (1977)

2 C

Orbital moment

Electron hybridization reduces m_L

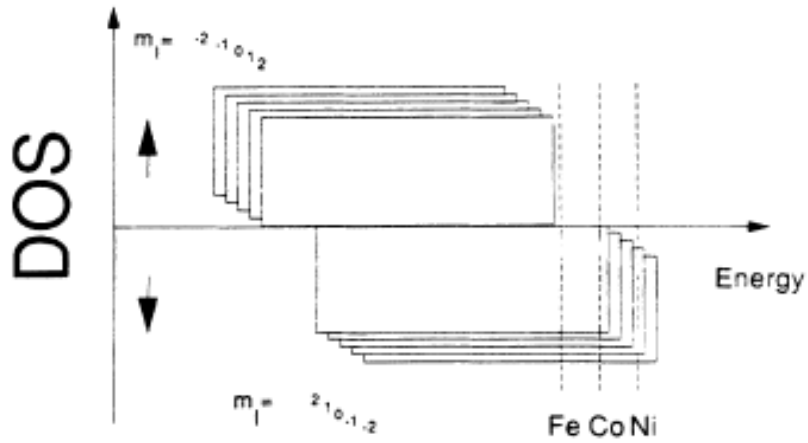

FIG. 2. Model state density for fcc Fe, Co, and Ni. Due to the spin-orbit coupling the degeneracy between the m_l and $-m_l$ states is lifted and an orbital moment develops. The correct number of valence electrons is obtained by adjusting the Fermi level as marked in the figure (Fe, Co, and Ni).

Eriksson et al., Phys. Rev. B 42, 2707 (1990).

	$\mathbf{m}_L$ atom (μ_B)	$\mathbf{m}_L$ bulk (μ_B)
Fe (-bcc)	2.0	0.09
Co (-hcp)	3.0	0.15
Ni (-fcc)	3.0	0.05

E.P. Wohlfart, in *Ferromagnetic Materials*, Vol. 1, E.P. Wohlfart ed., North Holland, Amsterdam (1980).

Cubic symmetry *d*-wavefunctions

$$\psi_1 \equiv d_{xz} = \sqrt{\frac{15}{4\pi}}\frac{xz}{r^2} = \frac{1}{\sqrt{2}}\left(-Y_{21} + Y_{2-1}\right)$$

$$\psi_2 \equiv d_{xy} = \sqrt{\frac{15}{4\pi}}\frac{xy}{r^2} = \frac{-i}{\sqrt{2}}\left(Y_{22} - Y_{2-2}\right)$$

$$\psi_3 \equiv d_{yz} = \sqrt{\frac{15}{4\pi}}\frac{yz}{r^2} = \frac{i}{\sqrt{2}}\left(Y_{21} + Y_{2-1}\right)$$

$$\psi_4 \equiv d_{3z^2-r^2} = \sqrt{\frac{5}{16\pi}}\frac{3z^2 - r^2}{r^2} = Y_{20}$$

$$\psi_5 \equiv d_{x^2-y^2} = \sqrt{\frac{5}{16\pi}}\frac{x^2 - y^2}{r^2} = \frac{1}{\sqrt{2}}\left(Y_{22} + Y_{2-2}\right)$$

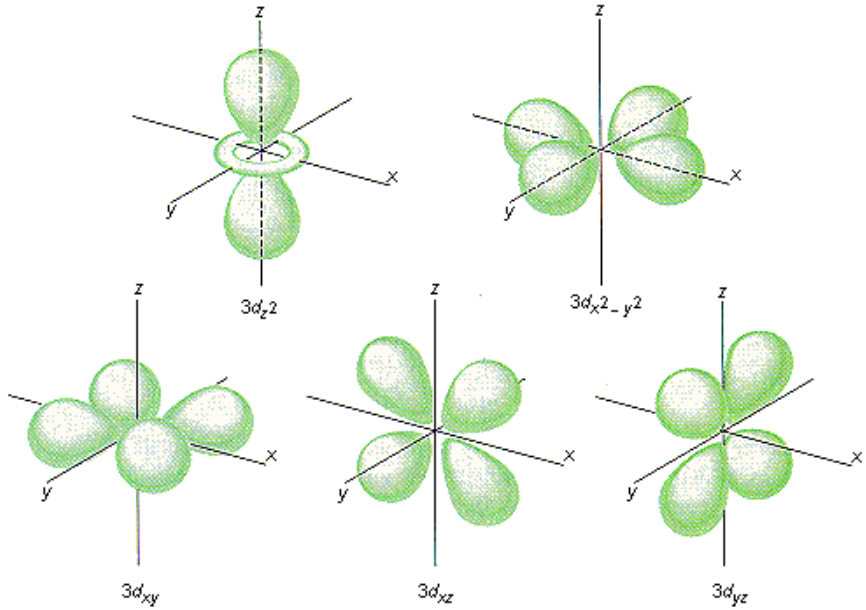

$$\boldsymbol{m}_L = -\mu_B \boldsymbol{L}$$

$$H_{Zeeman} = -\boldsymbol{m}_L \cdot \mathbf{B} = \mu_B L_z B$$

Electrons described by real 3*d* wavefunctions have zero orbital moment:

$$\langle\psi_5|\mathbf{L}_z|\psi_5\rangle = \frac{1}{2}\left(\langle+2| + \langle-2|\right)\mathbf{L}_z\left(|+2\rangle + |-2\rangle\right) = \frac{1}{2}\left(+2-2\right) = 0$$

Orbital moment in a cubic crystal field

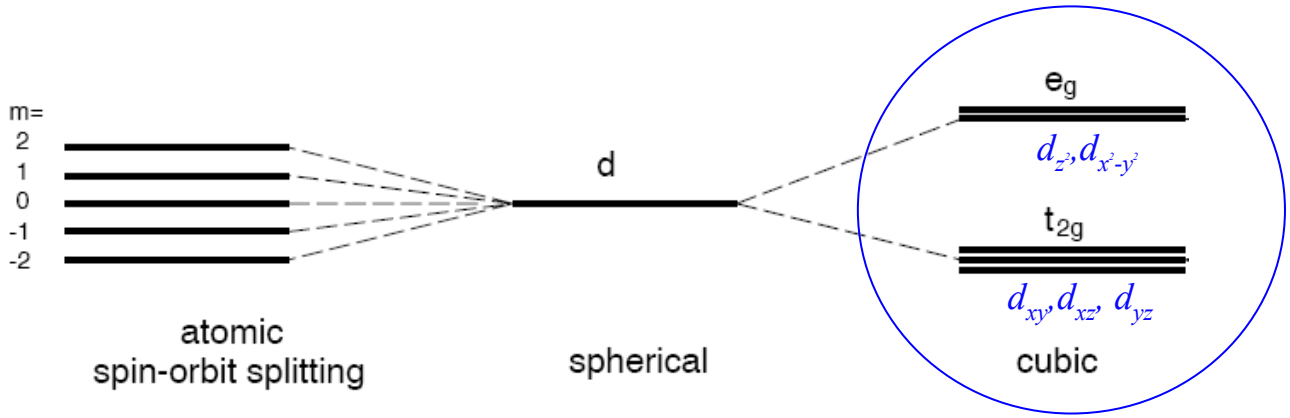

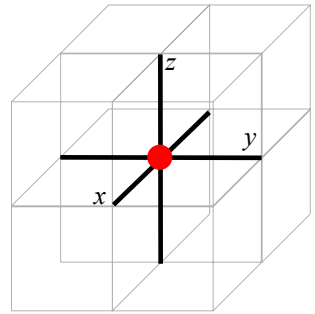

In the presence of a cubic crystal field larger than the s.o. or Zeeman field:

t_{2g} subspace:

$$\langle L_z \rangle_{ij} = \begin{pmatrix} 0 & 0 & -i \\ 0 & 0 & 0 \\ i & 0 & 0 \end{pmatrix} \xrightarrow{\text{diagonalize}} \begin{pmatrix} -1 & 0 & 0 \\ 0 & 1 & 0 \\ 0 & 0 & 0 \end{pmatrix}$$

eigenvectors

$$t_1 = \frac{1}{\sqrt{2}}(\psi_1 - i\psi_3) = Y_{2-1}$$

$$t_2 = \frac{1}{\sqrt{2}}(-i\psi_1 + \psi_3) = Y_{21}$$

$$t_3 = \psi_2 = \frac{-i}{\sqrt{2}}(Y_{22} - Y_{2-2})$$

Partial quench

e_g subspace:

$$\langle L_z \rangle_{ij} = \begin{pmatrix} 0 & 0 \\ 0 & 0 \end{pmatrix}$$

$$e_1 = \psi_4 = Y_{20}$$

$$e_2 = \psi_5 = \frac{1}{\sqrt{2}}(Y_{22} + Y_{2-2})$$

Total quench

unperturbed Schroedinger equation: $\mathrm{H}_0 \left|\psi^0_{gnd}\right\rangle = E^0_{gnd} \left|\psi^0_{gnd}\right\rangle$

small perturbation: $(\mathrm{H}_0 + \lambda \mathrm{V})\left|\psi\right\rangle = E\left|\psi\right\rangle$

$$E = E^{(0)} + \lambda E^{(1)} + \lambda^2 E^{(2)} + \ldots,$$

$$\left|\psi\right\rangle = \left|\psi^{(0)}\right\rangle + \lambda\left|\psi^{(1)}\right\rangle + \lambda^2\left|\psi^{(2)}\right\rangle + \ldots$$

$$E^{(1)} = \left\langle \psi^{(0)}_{gnd} \middle| V \middle| \psi^{(0)}_{gnd} \right\rangle$$

$$\left|\psi^{(1)}\right\rangle = \sum_{\mathrm{exc}\neq\mathrm{gnd}} \frac{\left\langle \psi^{(0)}_{exc} \middle| V \middle| \psi^{(0)}_{gnd} \right\rangle}{E^{(0)}_{exc} - E^{(0)}_{gnd}} \left|\psi^{(0)}_{exc}\right\rangle$$

$$E^{(2)} = \sum_{\mathrm{exc}\neq\mathrm{gnd}} \frac{\left|\left\langle \psi^{(0)}_{exc} \middle| V \middle| \psi^{(0)}_{gnd} \right\rangle\right|^2}{E^{(0)}_{exc} - E^{(0)}_{gnd}}$$

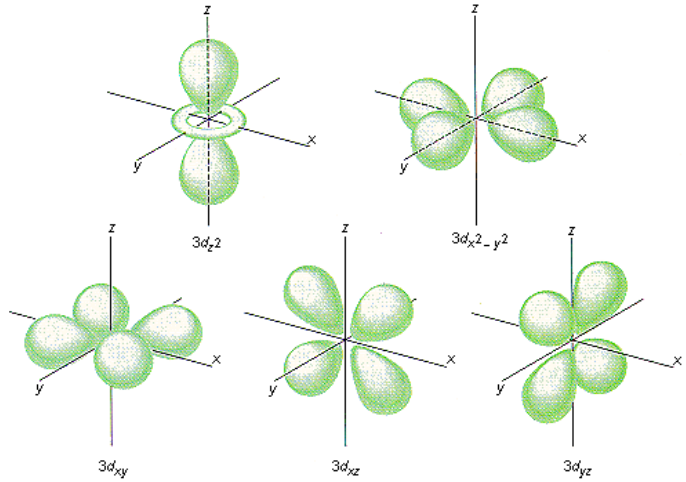

$$\lambda V = \lambda \mathbf{L}\cdot\mathbf{S}$$

$$\left\langle \mathbf{L} \right\rangle_{\mathrm{gnd}} = \left\langle \psi^{(0)}_{gnd} \middle| \mathbf{L} \middle| \psi^{(0)}_{gnd} \right\rangle = 0$$

$$\left\langle \mathbf{L} \right\rangle = \left\langle \psi \middle| \mathbf{L} \middle| \psi \right\rangle \approx \sum_{\mathrm{exc}\neq\mathrm{gnd}} \frac{\left\langle \psi^{(0)}_{exc} \middle| \lambda\mathbf{L}\cdot\mathbf{S} \middle| \psi^{(0)}_{gnd} \right\rangle}{E^{(0)}_{exc} - E^{(0)}_{gnd}} \left\langle \psi^{(0)}_{gnd} \middle| \mathbf{L} \middle| \psi^{(0)}_{exc} \right\rangle \neq 0$$

Tetragonal distorted d^9 state (Cu^{2+} , 10 Dq=2 eV, D_s=0.1 eV, D_t = 0)

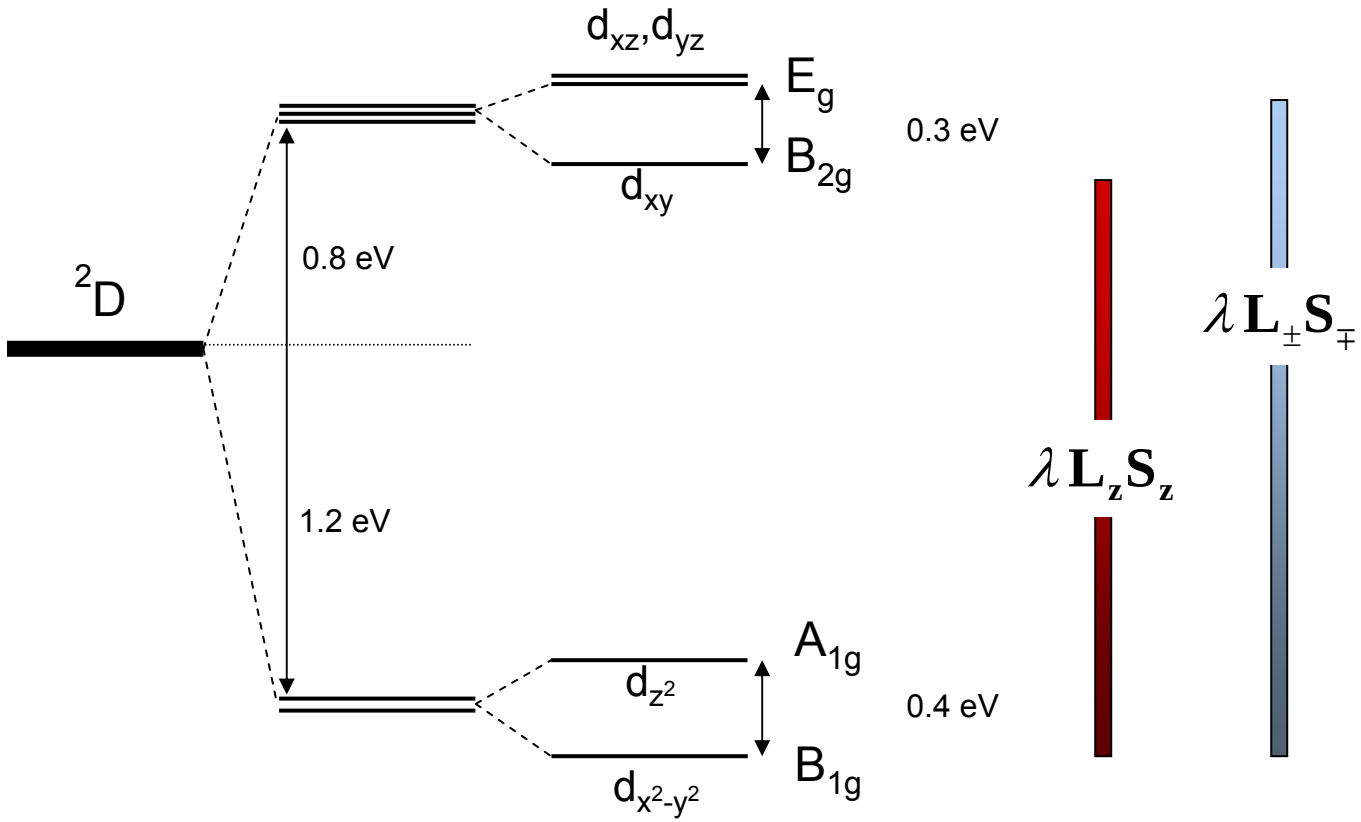

Unperturbed ground state has d_{x2-y2} symmetry, i.e., <L> = 0, however

$$\lambda \mathbf{L}\cdot\mathbf{S} = \lambda\left(\mathbf{L}_z\mathbf{S}_z + \mathbf{L}_+\mathbf{S}_- + \mathbf{L}_-\mathbf{S}_+\right)$$

mixes excited states into d_{x2-y2} inducing nonzero <L> ~ $\lambda/\Delta E$

Orbital d-shell moment in an atom

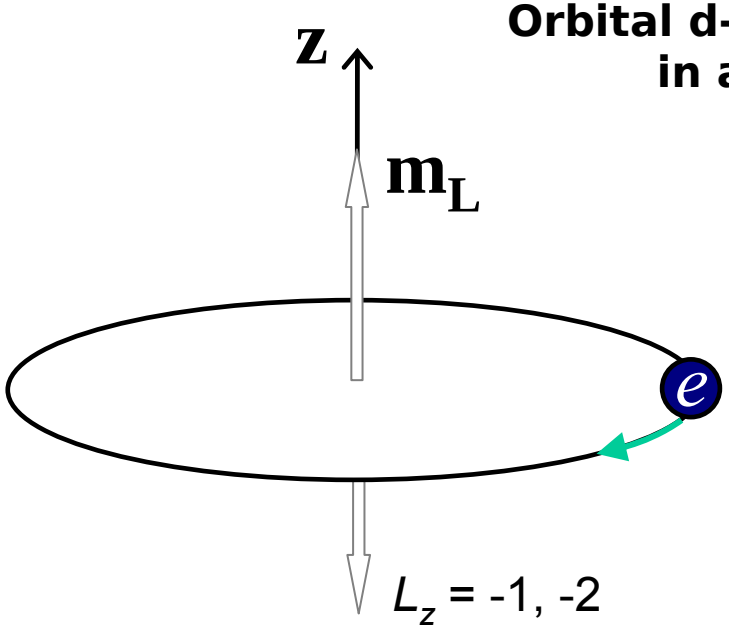

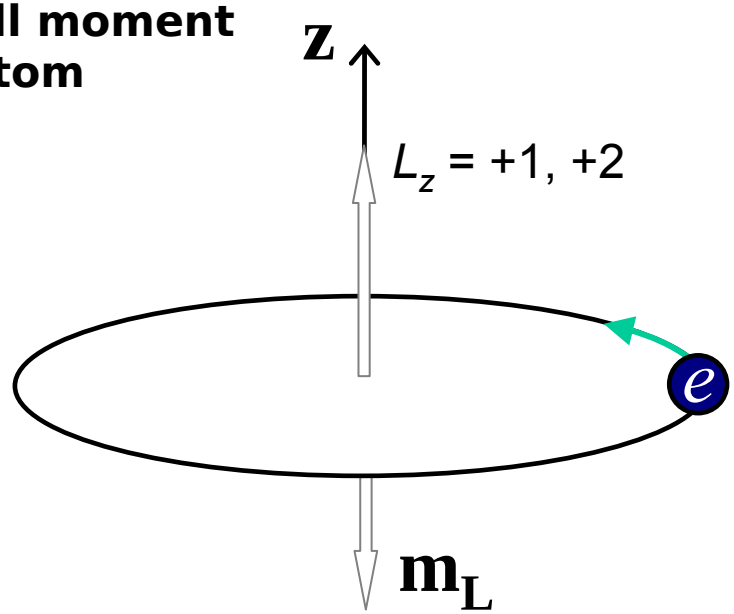

Directional quenching of orbital moment in a free-standing metal layer:

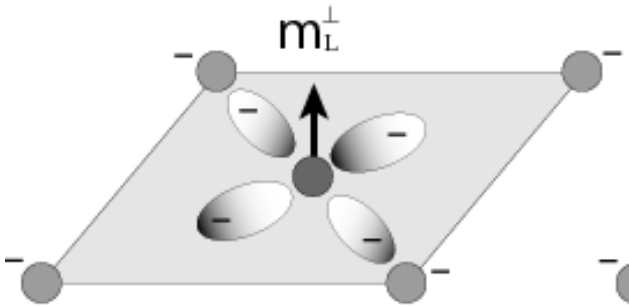

$$d_{xy} \sim |+2\rangle - |-2\rangle$$

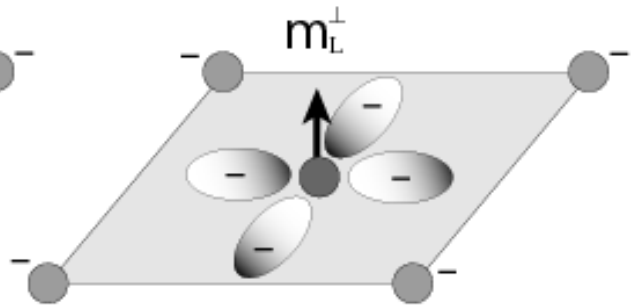

$$d_{x^2-y^2} \sim |+2\rangle + |-2\rangle$$

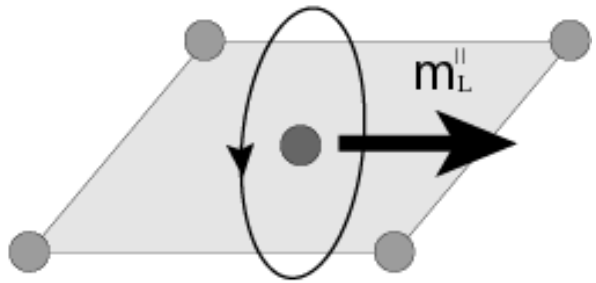

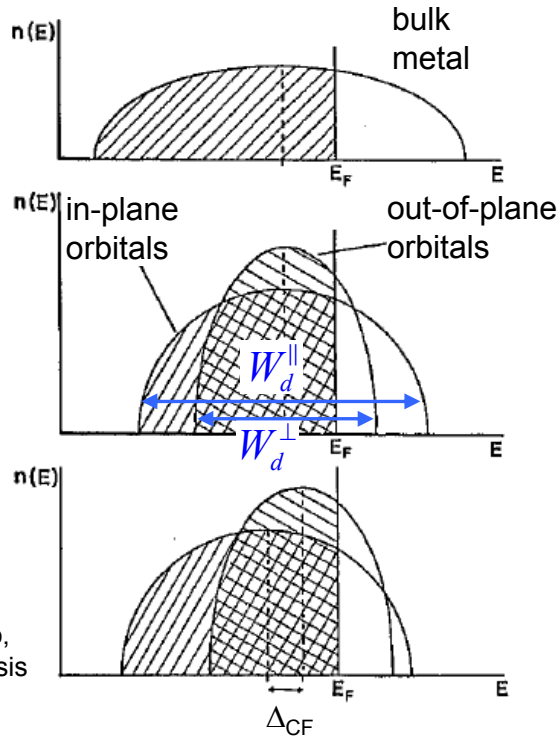

P. Bruno, PhD thesis

Band Narrowing

↓

Different in-plane and out-of-plane bandwidth

$$\Delta_{CF} = E(d_{xz}, d_{yz}, d_{3z^2-r^2}) - E(d_{xy}, d_{x^2-y^2})$$

Free-standing metal layer

$$m_L^{\perp} \propto \frac{1}{W_d^{\parallel}}$$

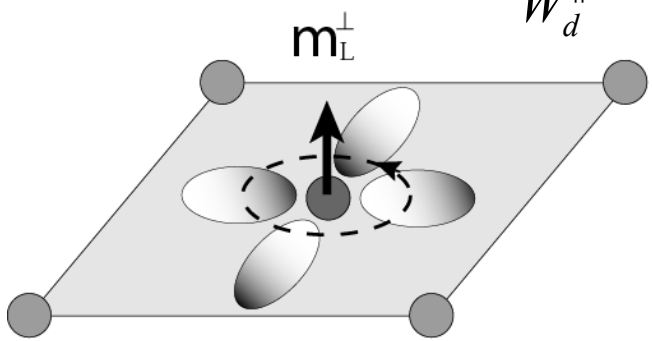

$$m_L^{\parallel} \propto \frac{1}{W_d^{\perp}}$$

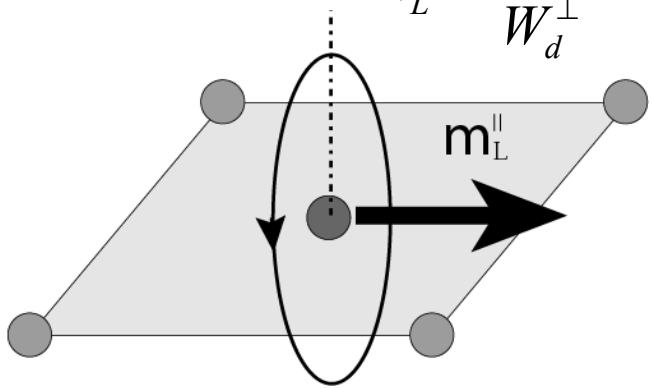

VOLUME 75, NUMBER 20 PHYSICAL REVIEW LETTERS 13 NOVEMBER 1995

Microscopic Origin of Magnetic Anisotropy in Au/Co/Au Probed with X-Ray Magnetic Circular Dichroism

D. Weller,[1] J. Stöhr,[1] R. Nakajima,[2] A. Carl,[1,*] M. G. Samant,[1] C. Chappert,[3] R. Mégy,[3] P. Beauvillain,[3] P. Veillet,[3] and G. A. Held[4]

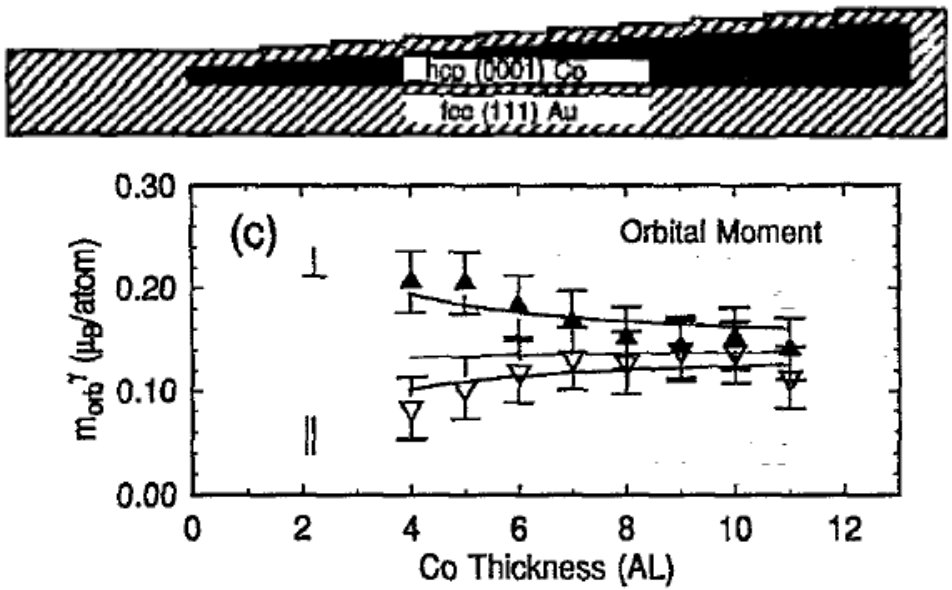

Co film free-standing $W_d^{\parallel} > W_d^{\perp} \Rightarrow m_L^{\perp} < m_L^{\parallel}$

Co film on Au $W_d^{\parallel} < W_d^{\perp} \Rightarrow m_L^{\perp} > m_L^{\parallel}$

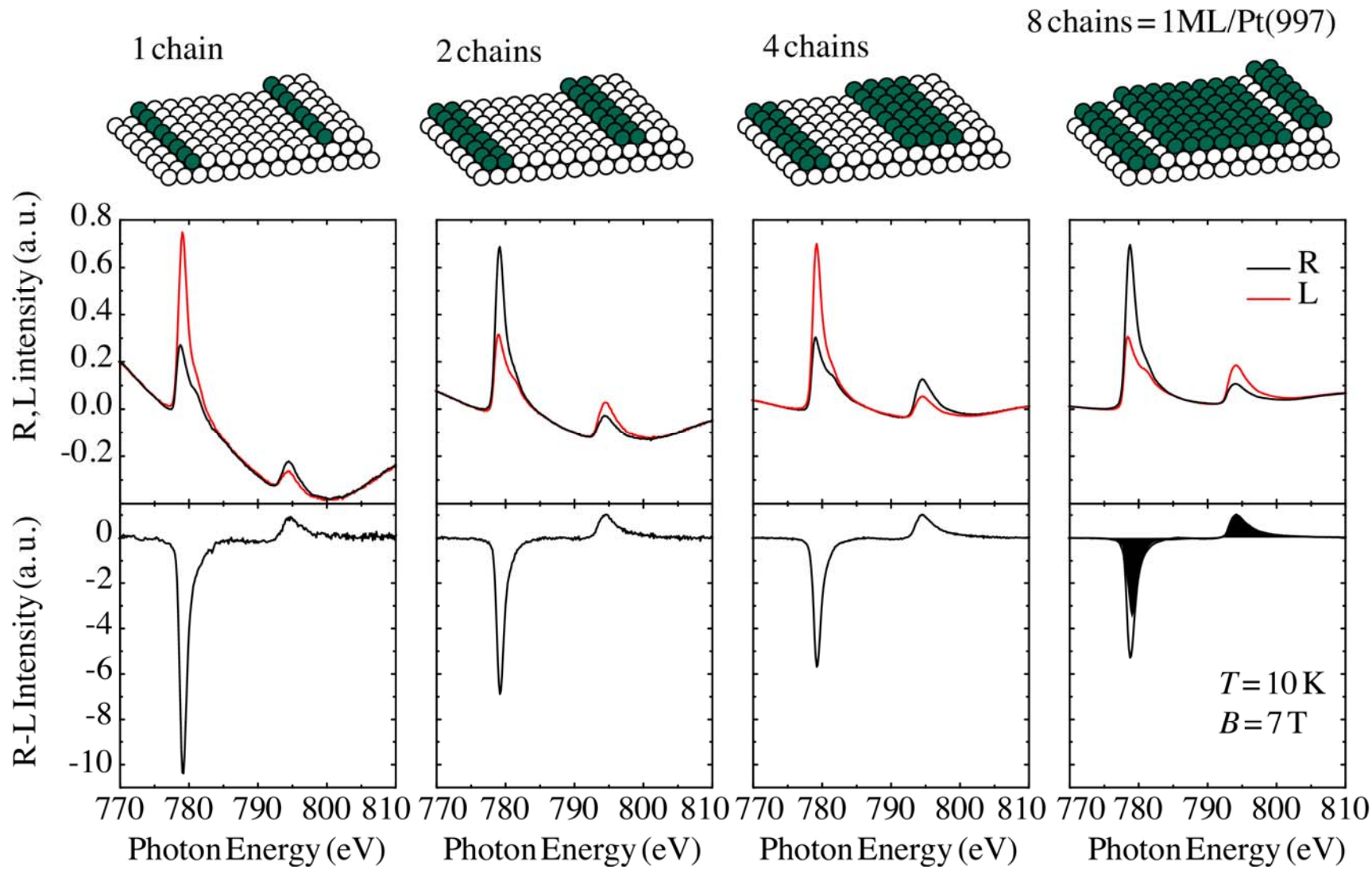

m_L 0.68 μ_B 0.37 μ_B 0.33 μ_B 0.31 μ_B

P. Gambardella et al., *Phys. Rev. Lett.* **93**, 077203 (2004).

crystal field → electron orbits → fixes **L** relative to the crystal lattice

Different **L** values along different crystal directions

Direction with the largest component of **L** → Lowest spin-orbit energy → easy direction of magnetization

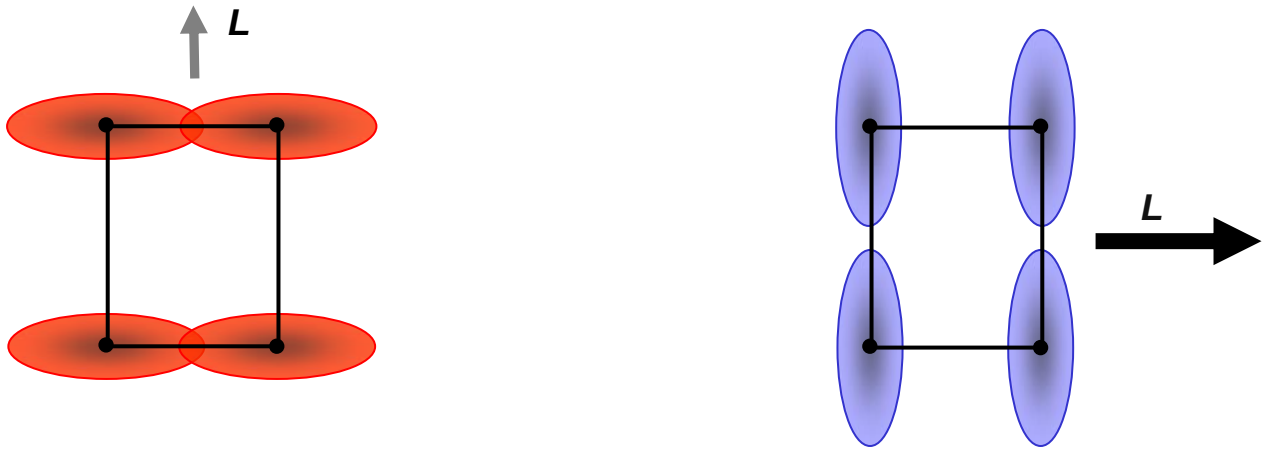

see, e.g., P. Bruno, PRB **39**, 865 (1989);
H. A. Dürr et al., *Science* **277**, 213 (1997).

3

Magnetocrystalline anisotropy

$$E_a = E(\mathbf{M} \parallel \hat{z}) - E(\mathbf{M} \perp \hat{z})$$

Can be defined as: magnetic anisotropy energy per atom (eV/atom)
magnetic anisotropy energy per unit volume (MJ/m^3, erg/cm^3)

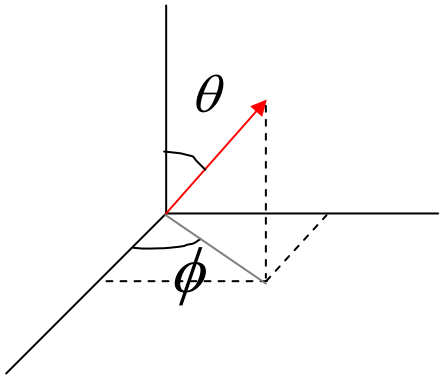

$$\alpha_1 = \cos\theta$$
$$\alpha_2 = \sin\theta\cos\phi$$
$$\alpha_3 = \sin\theta\sin\phi$$

cubic system:

$$\begin{aligned} F(\mathbf{M}) &= K_0 + K_1(\alpha_1^2\alpha_2^2 + \alpha_1^2\alpha_3^2 + \alpha_2^2\alpha_3^2) + K_2\alpha_1^2\alpha_2^2\alpha_3^2 + \ldots \\ &= K_0 + \frac{K_1}{64}\{(3 - 4\cos 2\theta + \cos 4\theta)(1 - \cos 4\phi) + 8(1 - \cos 4\theta)\} + \\ &\quad + \frac{K_2}{256}(1 - \cos 2\theta - 2\cos 4\theta + \cos 6\theta)(1 - \cos 4\phi) + \ldots \end{aligned}$$

uniaxial system:

$$F(\mathbf{M}) = K_0 + K_1\sin^2\theta + K_2\sin^4\theta + \ldots$$

Fe bcc

easy axis: (100)

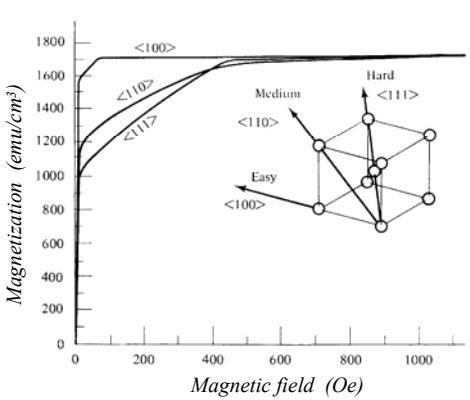

$K_1 = 4.8 \times 10^4 \ J/m^3$

$= 2.4 \ \mu eV / atom$

Co hcp

easy axis: (0001)

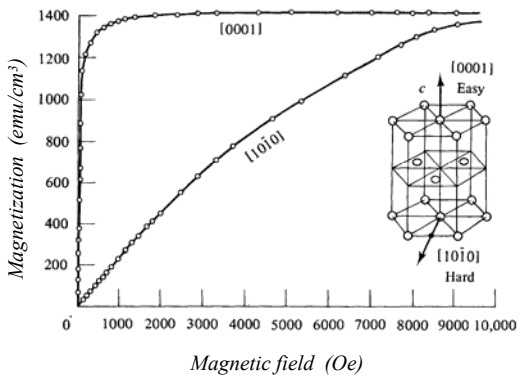

$K_1 = 4.1 \times 10^5 \ J/m^3$

$= 45 \ \mu eV / atom$

Ni fcc

easy axis: (111)

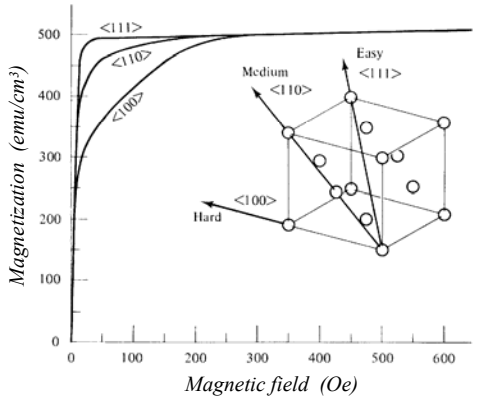

$K_1 = -5.5 \times 10^3 \ J/m^3$

$= -0.3 \ \mu eV / atom$

S. Kaya, *Sci. Reports Tohoku Univ.* 17, 639 (1928)

$F(\theta,\phi,K_1>0)$

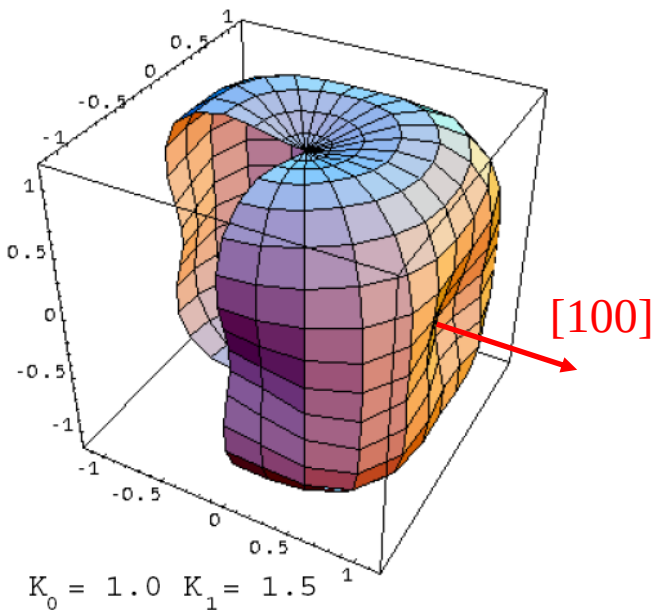

$F(\theta,\phi,K_1<0)$

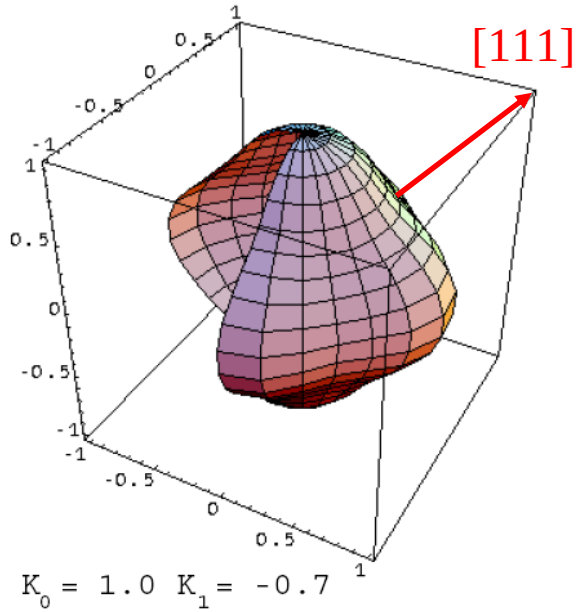

Table 1: *Typical ground-state energies E in eV/atom for 3d metal films*

	E (eV/atom)
cohesive energy	5.5
local moment formation	1.0
alloy formation	0.5
magnetic order	0.2
structural relaxation	0.05
magnetic anisotropy	0.0001÷0.002

Courtesy G. Bihlmayer, FZ Jülich

Temperature dependence of magnetic anisotropy energy constants

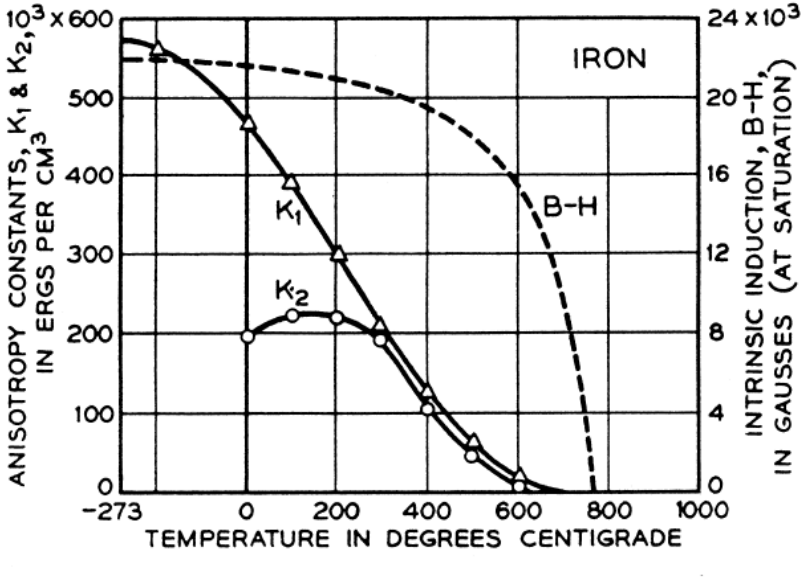

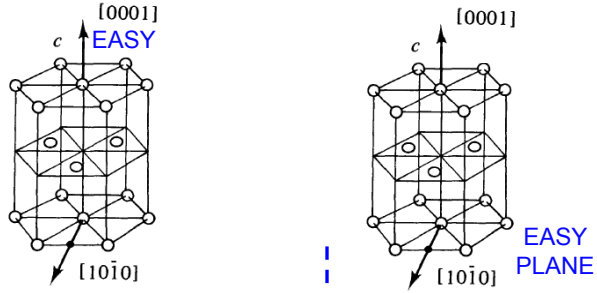

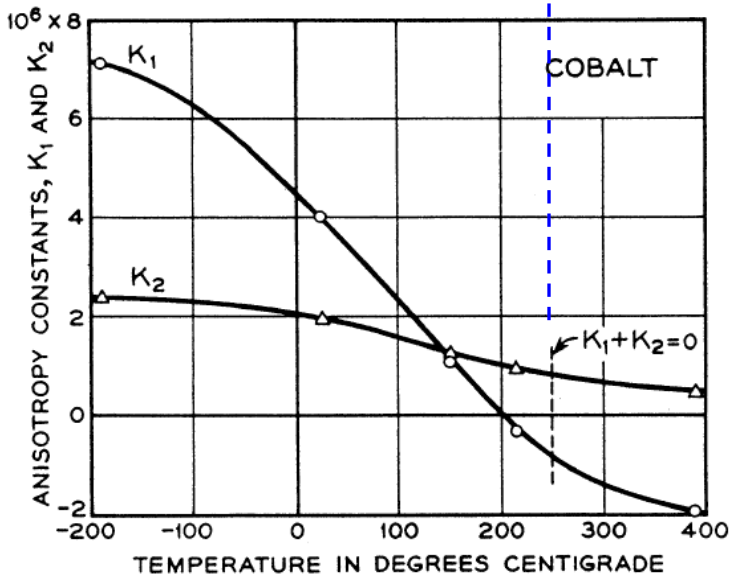

Tome 15. N° 4. Avril 1954.

LE JOURNAL DE PHYSIQUE
ET
LE RADIUM

ANISOTROPIE MAGNÉTIQUE SUPERFICIELLE ET SURSTRUCTURES D'ORIENTATION

Par M. Louis NÉEL,
Laboratoire d'Électrostatique et de Physique du Métal, Grenoble.

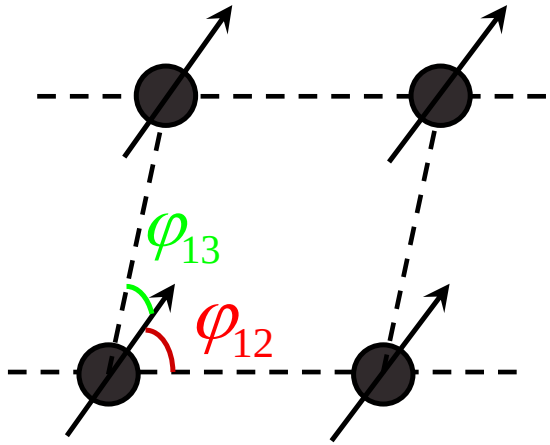

The magnetocristalline energy term depends on the symmetry of the crystal which defines the interaction directions between neighbour atoms. In a classic pair model the energy of a pair of atoms is supposed to depend only on the angle between their spins and the interatomic axis:

$$E_{ij} = l(\cos^2 \varphi_{ij} - 1/3) + q(\cos^4 \varphi_{ij} + \ldots)$$

For a solid with cubic simmetry, summing E_{ij} over nearest neighbours cancels out the $\cos^2$ term this is not true anymore in the case of a surface, where the anisotropy energy per unit area becomes (neglecting the higher order terms):

$$K = \frac{1}{2}\sum_{i,j} l \cos^2 \varphi_{ij}$$

Effective anisotropy constants in magnetic thin films

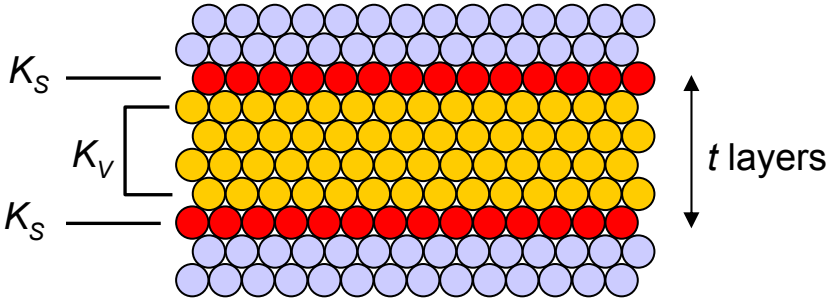

$$K_{Co}^{eff} = \left(K_{Volume} - 2\pi M_0^2\right) + 2K_{Surface}/t_{Co}$$

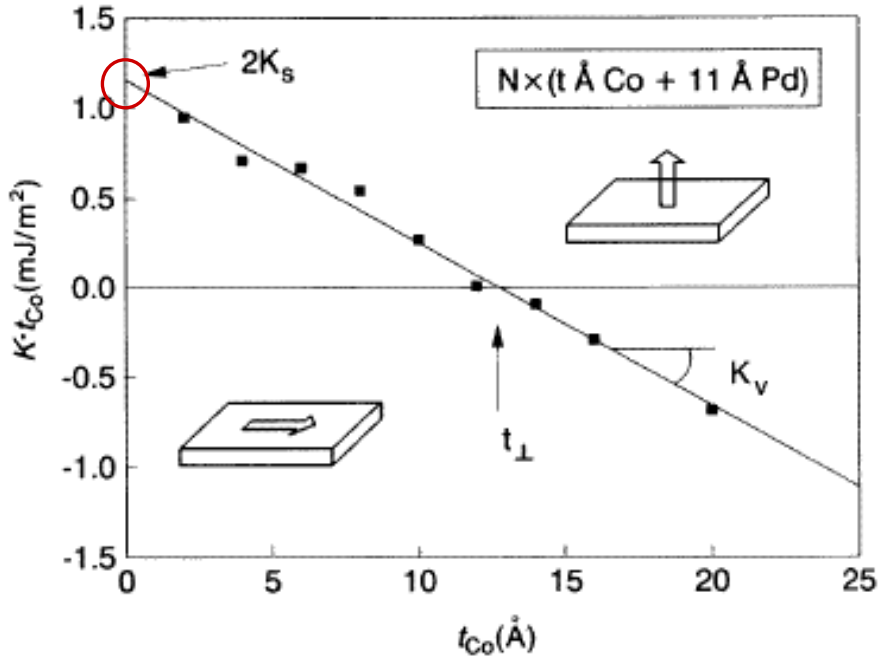

W. J. M. de Jonge et al., in Ultrathin Magnetic Structures I, J. A. C. Bland and B. Heinrich eds., Springer (1994)

Au/Co(t)/Au T = 10 K

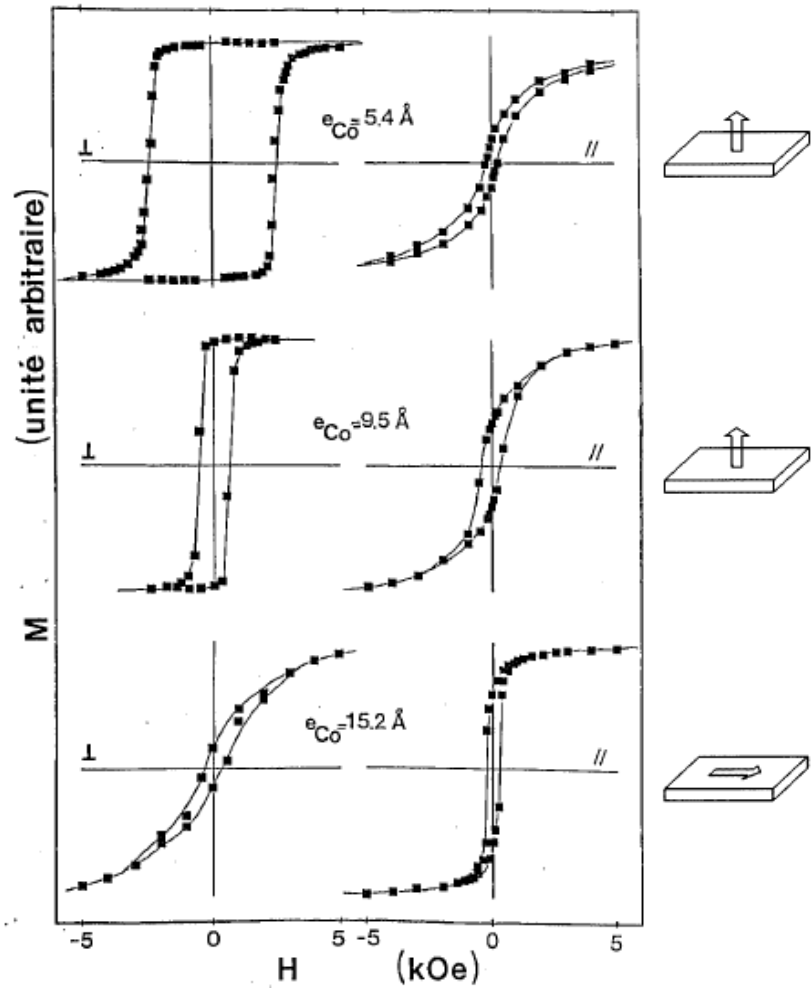

Chappert and Bruno, J. Appl. Phys. 64, 5736 (1988)

Out-of-plane to in-plane spin reorientation above threshold thickness

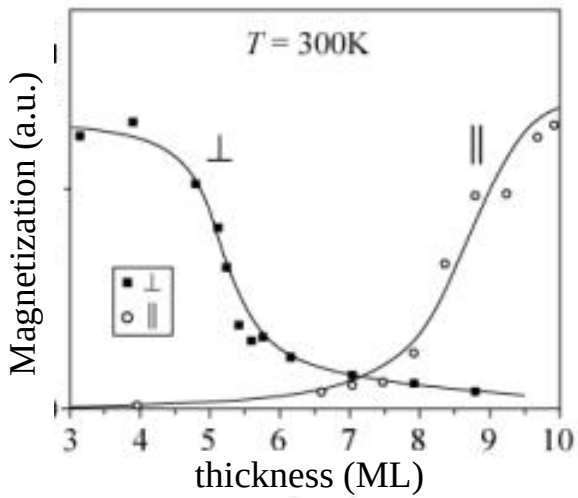

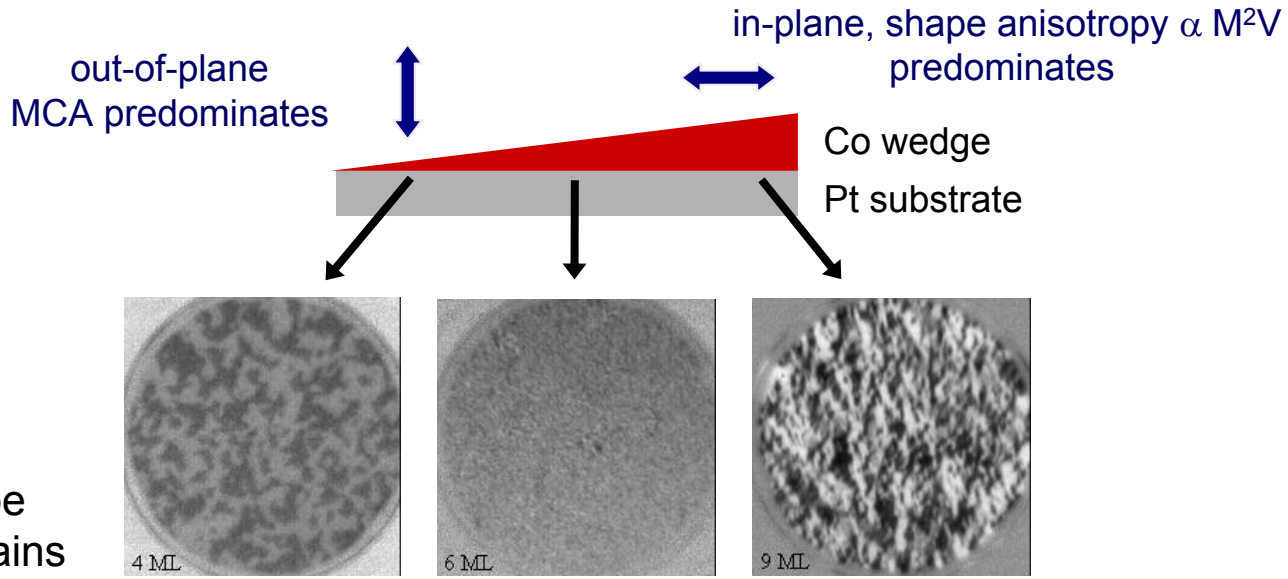

Orientation and shape
of Co magnetic domains

S. Rusponi, P.G., L. Claude, H. Brune, F. Nolting, unpublished

PHYSICAL REVIEW B VOLUME 42, NUMBER 17 15 DECEMBER 1990-I

Molecular-beam-epitaxial growth and magnetic properties of Co-Pt superlattices oriented along the [001], [110], and [111] axes of Pt

C. H. Lee, R. F. C. Farrow, C. J. Lin, and E. E. Marinero
IBM Research Division, Almaden Research Center, 650 Harry Road, San Jose, California 95120-6099

C. J. Chien
Department of Materials Science and Engineering, Stanford University, Stanford, California 94305

Co/Pt superlattices grown by MBE with [001], [110], [111] orientation:

"Epitaxy along these different orientations can clearly induce defect structures and local lattice distortions that may result in different values of the magnetocrystalline anisotropy."

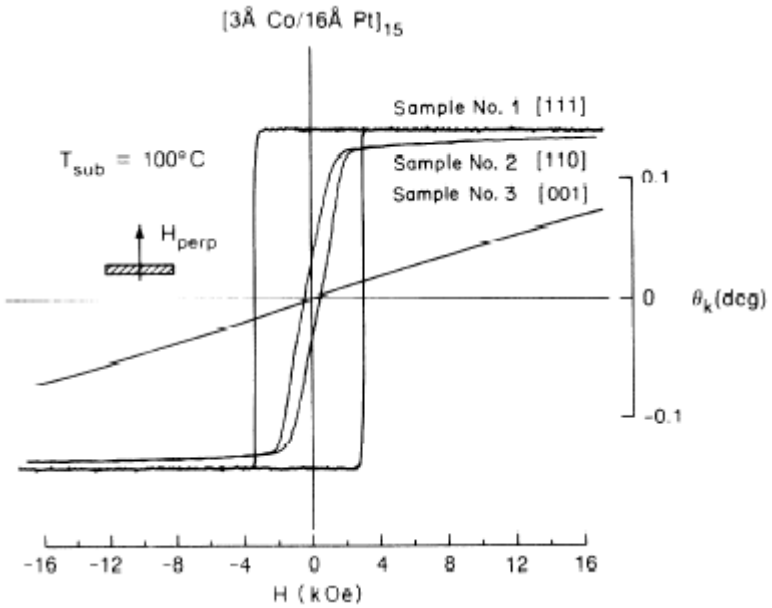

$$H_{so} = \xi\, \mathbf{S}\cdot\mathbf{L}$$

$$E_a = E_{so}(\hat{\mathbf{S}}_z) - E_{so}(\hat{\mathbf{S}}_x)$$

MODEL:
Bruno, PRB 1989

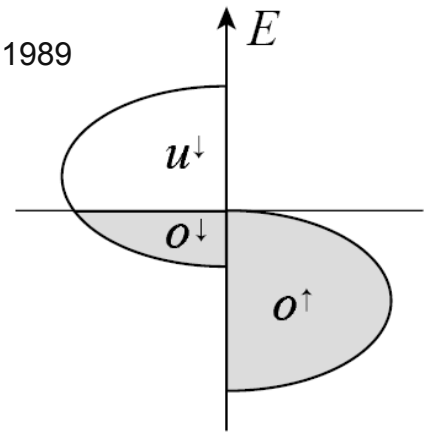

Only unoccupied states matter

$$E_{so}^{\downarrow\downarrow}(\hat{\mathbf{S}}) = \frac{\xi^2}{4}\sum_{o\downarrow,u\downarrow}\frac{|\langle o\downarrow|\mathbf{S}\cdot\mathbf{L}|u\downarrow\rangle|^2}{\epsilon_{o\downarrow}-\epsilon_{u\downarrow}}$$

$$E_a = E_{so}^{\downarrow\downarrow}(\hat{\mathbf{S}}_z) - E_{so}^{\downarrow\downarrow}(\hat{\mathbf{S}}_x) = \frac{\xi^2}{4}\sum_{o\downarrow,u\downarrow}\frac{|\langle o\downarrow|L_z|u\downarrow\rangle|^2 - |\langle o\downarrow|L_x|u\downarrow\rangle|^2}{\epsilon_{o\downarrow}-\epsilon_{u\downarrow}}$$

$$\langle L_{x,z}\rangle = \sum_{o,u}\langle o|L_{x,z}|u\rangle\frac{\langle u|H_{so}|o\rangle}{\epsilon_o-\epsilon_u}$$

$$E_a = \frac{\xi}{4}\left[\langle L_z\rangle - \langle L_x\rangle\right] = -\frac{\xi}{4\mu_B}\left[m_L^{\perp} - m_L^{\parallel}\right]$$

… a long story

1930s – Bloch and Gentile, Van Vleck

1940s – H. Brooks

…

Crystal field theory (see, e.g., Molecular Magnetism by O. Kahn)

…

1990s – transition metal films

P. Bruno, PRB 39, 865 (1989)

G. van der Laan, JPCM 10, 3239 (1998).

Magnetism of individual surface adatoms: $Co_1/Pt(111)$

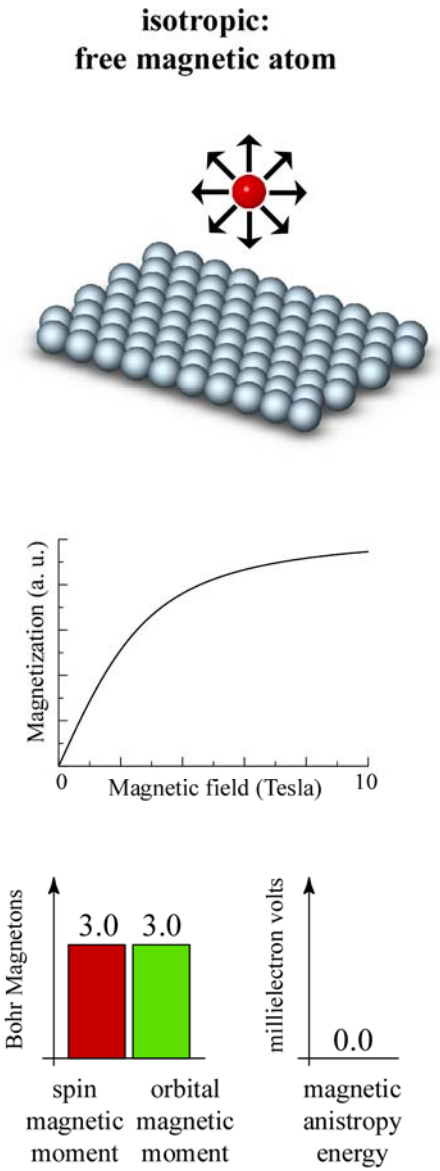

Factors that determine the magnetic anisotropy:

Angular dependence

- atomic symmetry

Magnitude

- 3*d* bandwidth
- orbital moment
- spin-orbit coupling

K depends on the atomic coordination:

$K_{Co_1/Pt} = 200\ K_{Co\ bulk}$

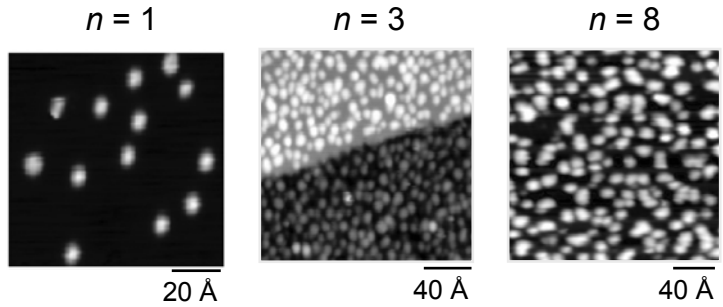

Co_n / Pt(111)
T = 5 K

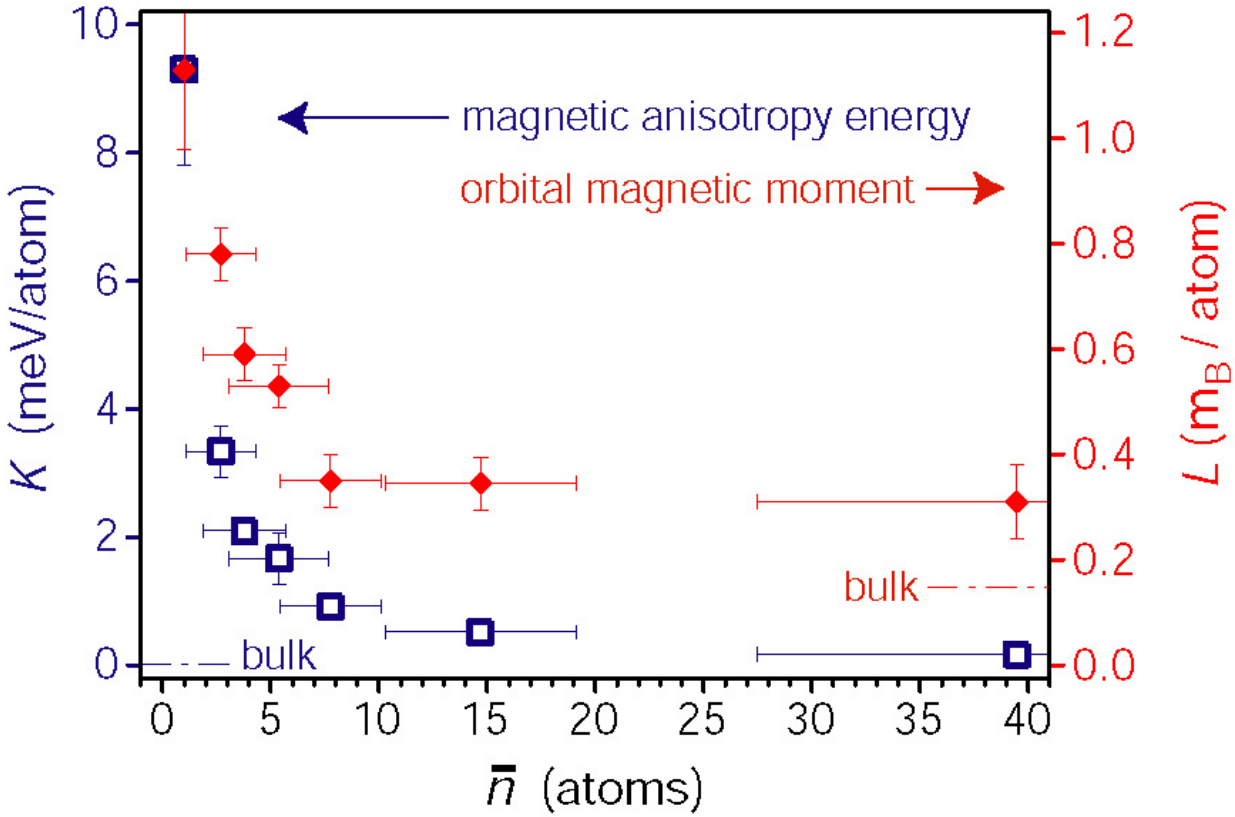

Science **300**, 1130 (2003)

Magnetization of individual surface adatoms: XMCD measurements

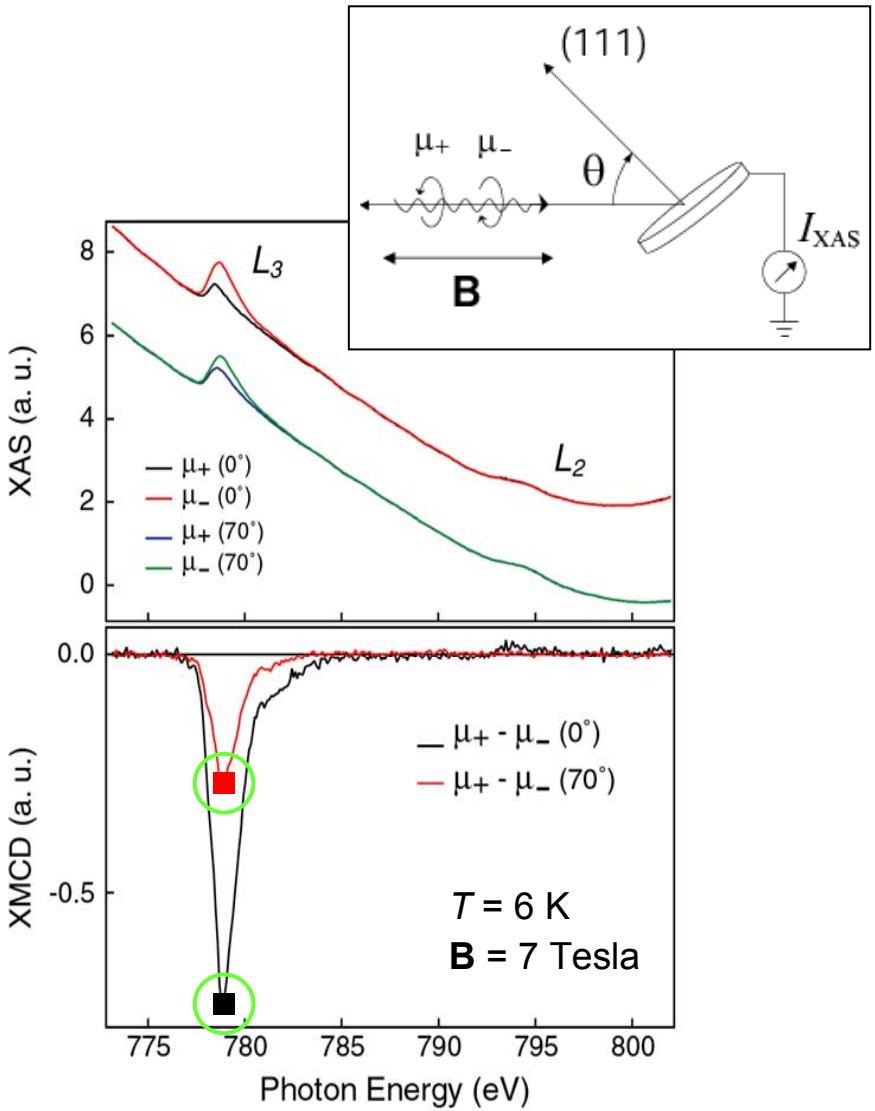

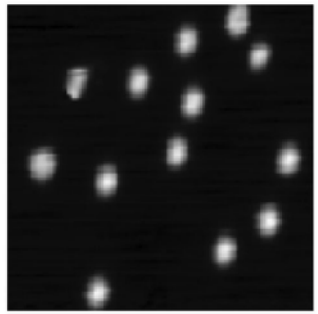

STM of individual Co atoms on Pt(111)
(image size 85 x 85 Å^2)

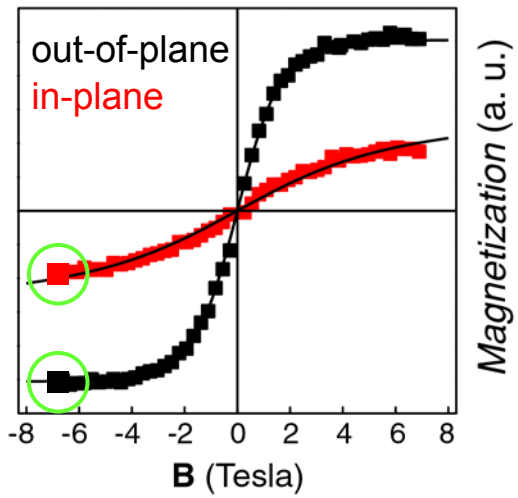

Science **300**, 1130 (2003); Surf. Sci. **603**, 1830 (2009).

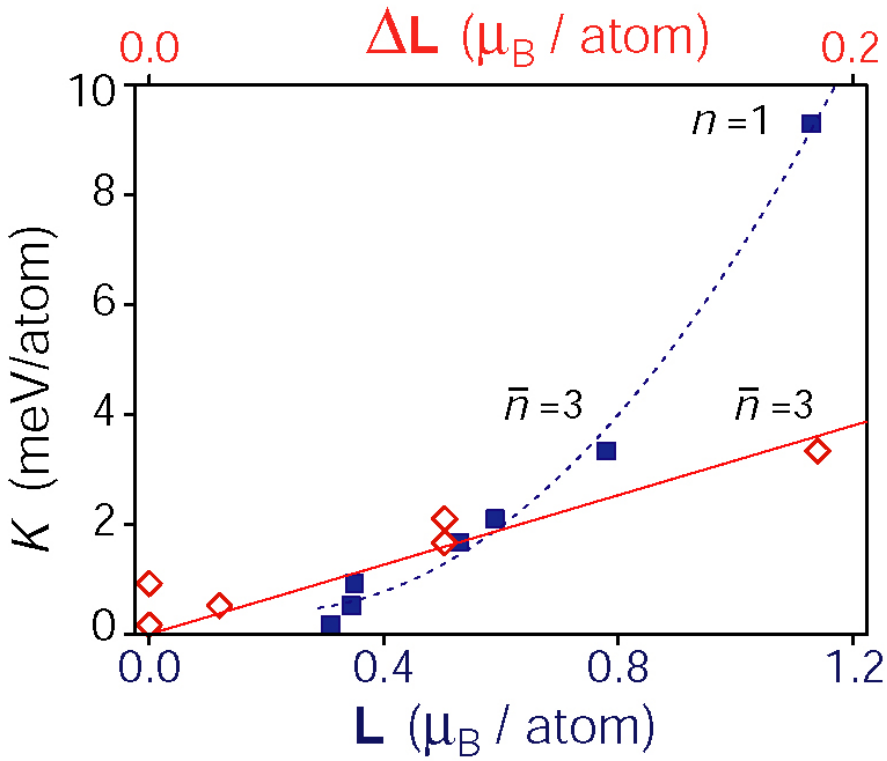

2nd order perturbation theory: P. Bruno, PRB 39, 865 (1989)
G. van der Laan, JPCM 10, 3239 (1998).

$$K \sim \frac{\xi_{\text{s.o.}}}{4} \langle \Delta \mathrm{L} \rangle$$

More on local atomic environment effects in metals

0.4 ML Co $T = 130$ K $T_{ann} = 300$ K

Monolayer
Co islands
Size about
1000 atoms

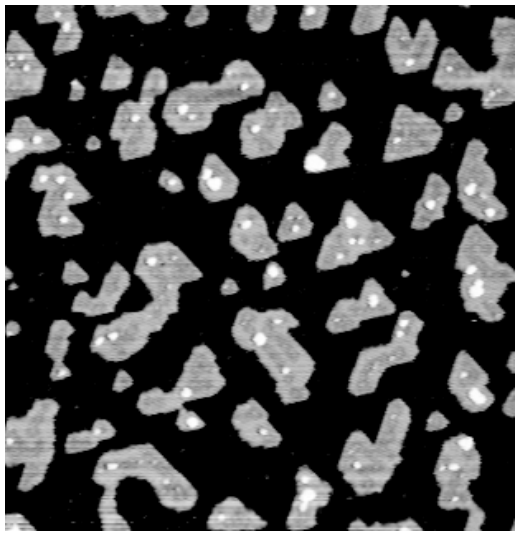

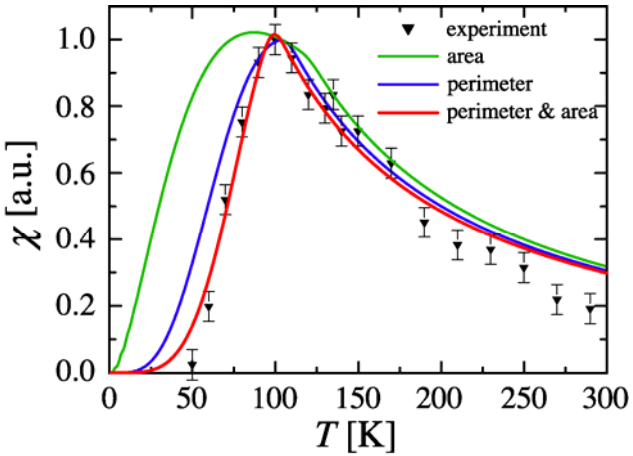

0. 2 ML Pt core
and 0.2 ML Co shell

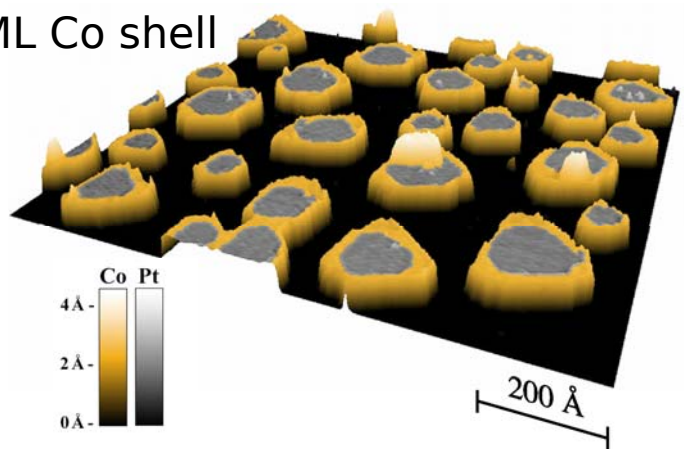

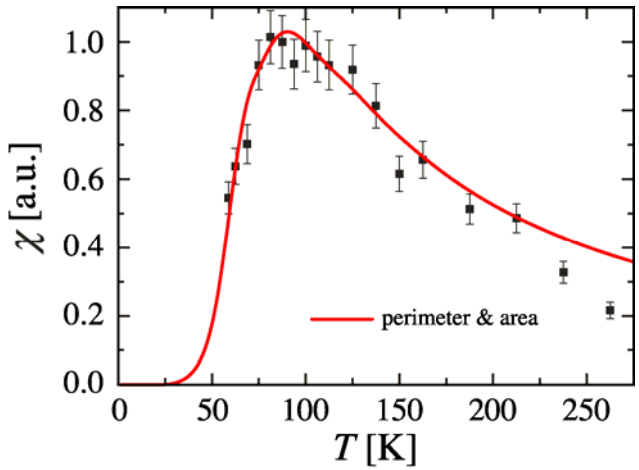

Compared to pure Co islands: 1) same total MAE
2) reduced magnetic moment

S. Rusponi *et al.*, Nature Mat. **2**, 546 (2003).

Nanomagnets: the ultimate size limit ?

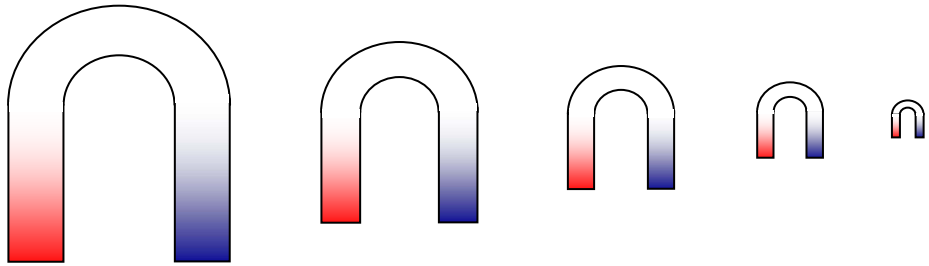

relaxation time of a magnetic particle: $\tau = \tau_0 \, e^{nK / k_B T}$

stability criterion: τ > 10 years

⇨ $nK / k_B T = 35$ @ $T = 350$ K ⇨ nK > 1 eV

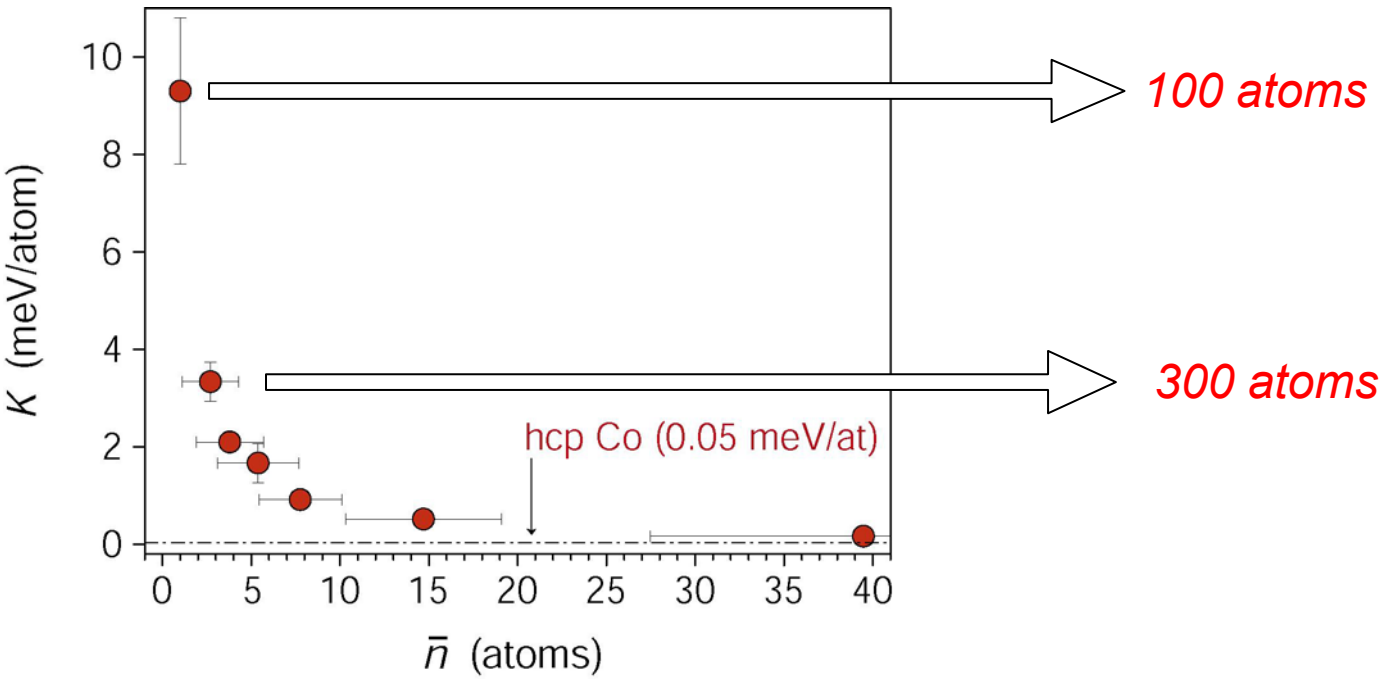

4

Single molecule magnets

Single-molecule magnets (SMMs)

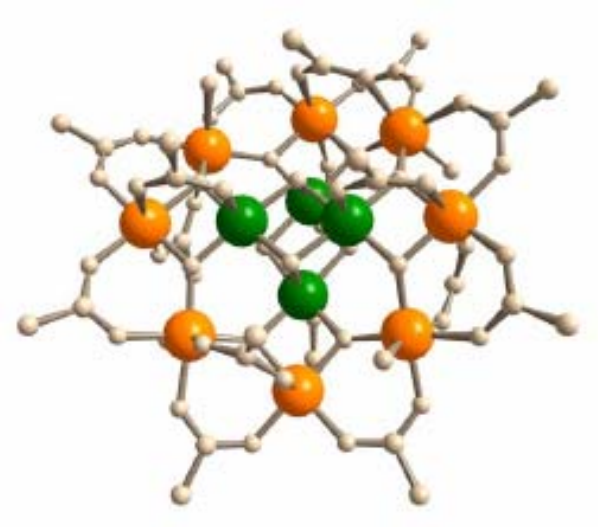

"Mn_{12} acetate"

Sessoli et al., Nature 1993

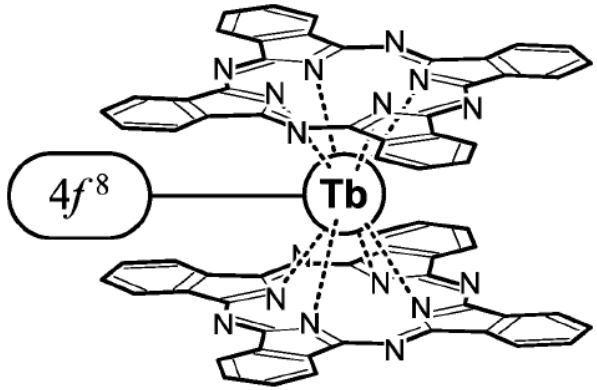

"Tb double-decker"

Ishikawa et al., JACS 2003

$$[Mn_{12}O_{12}(CH_3COO)_{16}(H_2O)_4]\cdot 2CH_3COOH\cdot 4H_2O$$

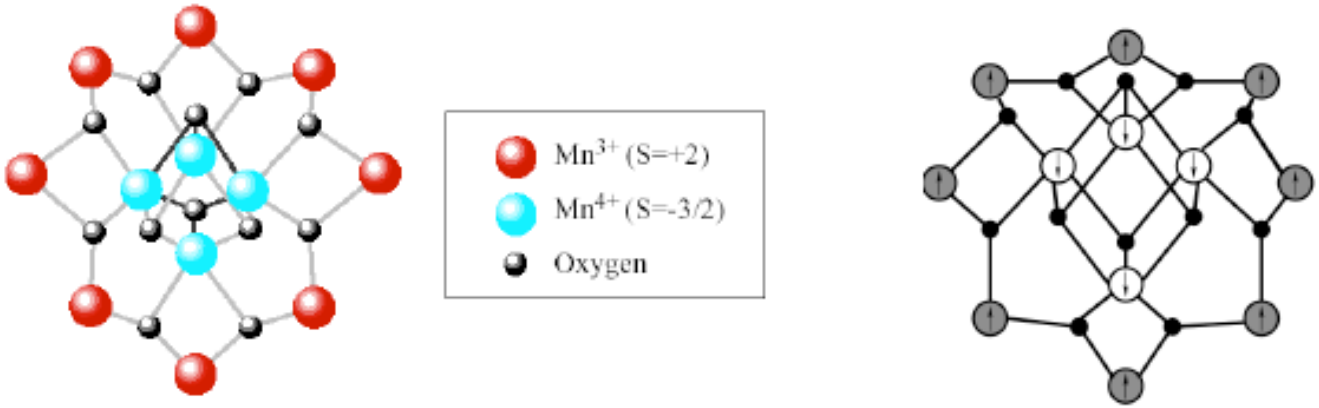

Total spin: **S=8x(2)+4x(-3/2)=10**

Spin Hamiltonian: $H = -DS_z^2 - AS_z^4 - g\mu_B S_z B_z$

Relatively large single molecule moment, 20 μ_B

Relatively small number of quantum levels

Magnetic relaxation at high temperature

Thermal activation (over the barrier)

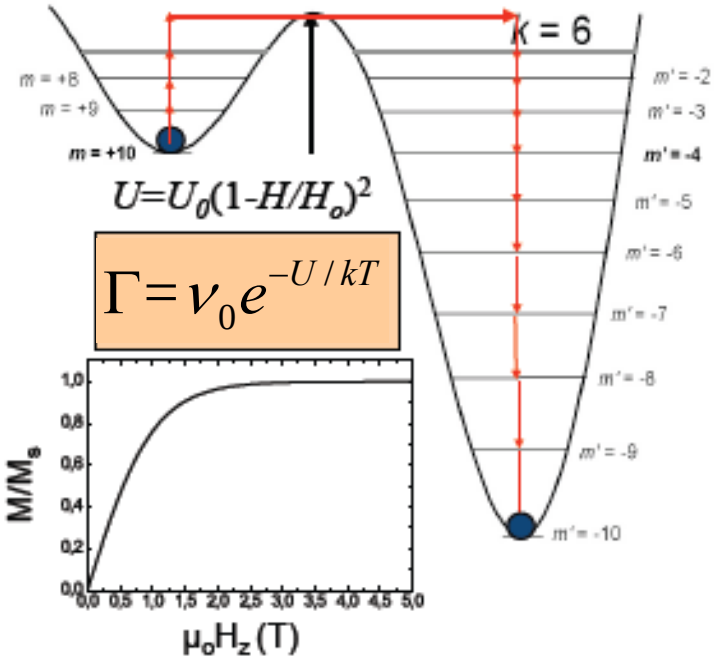

$$U = DS^2 + AS^4 = 6 \text{ meV}$$

and $\nu_0 = 0.5 \times 10^7 \text{ Hz}$

Arrhenius law

J.R. Friedman et al., PRL (1996)
L. Thomas et al., Nature, (1996)

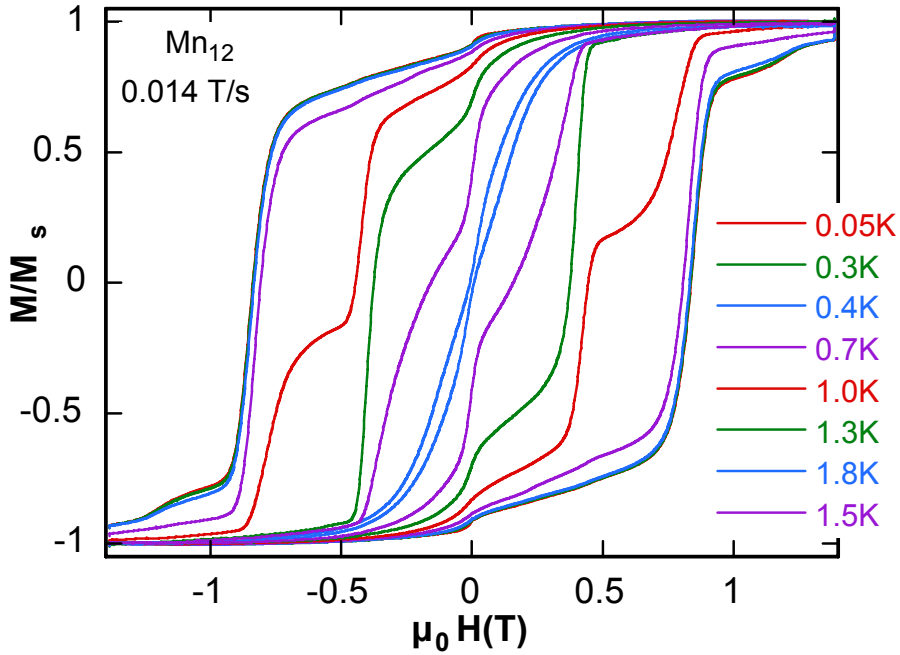

Classicaly :

Calculated field required to reverse the magnetization ≈ 12 T

Quantum tunneling between resonant spin states

Mn_{12} Molecular clusters

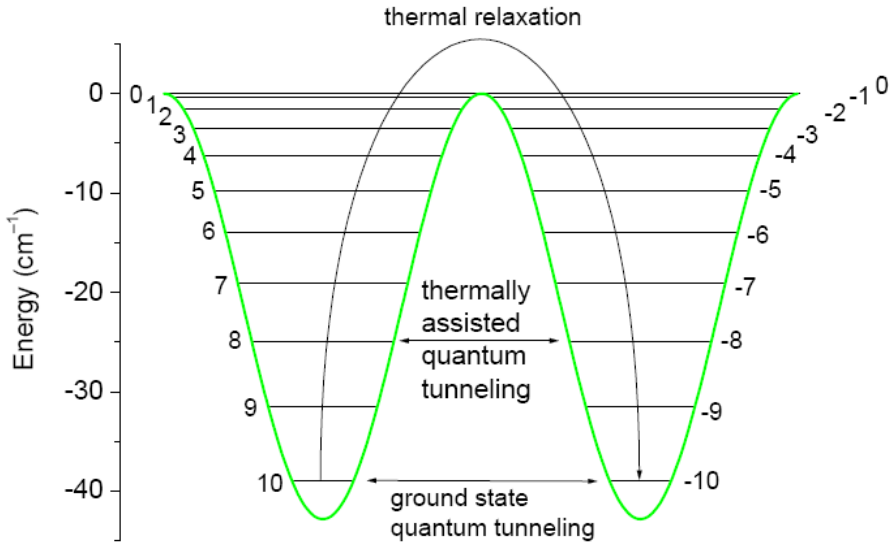

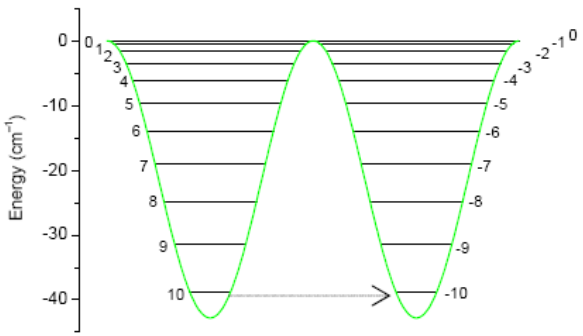

B =0

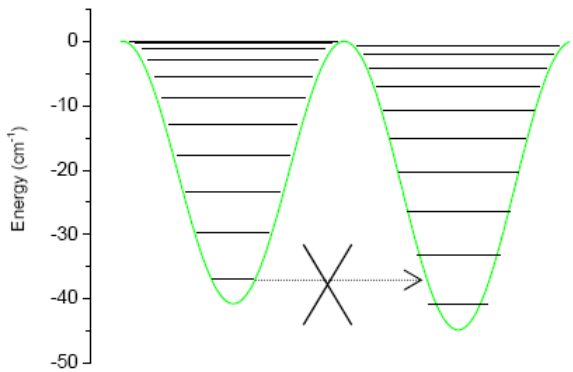

B≠0

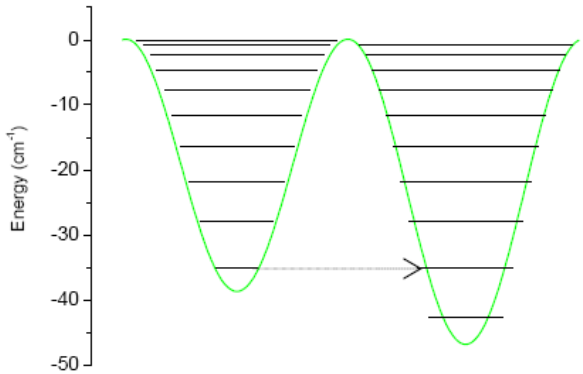

B≠0

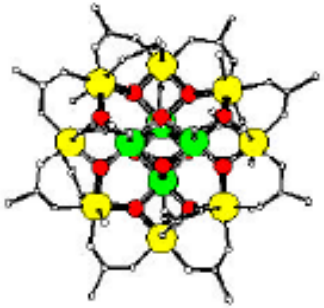

Mn_{12} (S = 10)

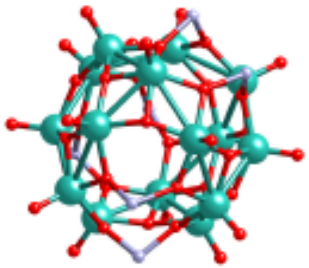

V_{15} (S = ½)

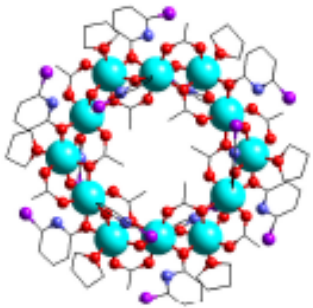

Ni_{12} (S = 12)

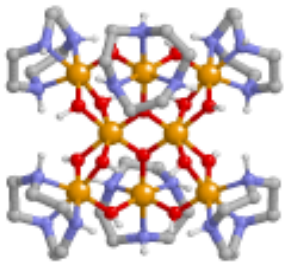

Fe_8 (S = 10)

- ✓ smalles magnets
- ✓ identical quantum objects
- ✓ cheap to make

- X low T_B
- X not easy to manipulate/assemble
- X write?

Surface functionalization of SMM?

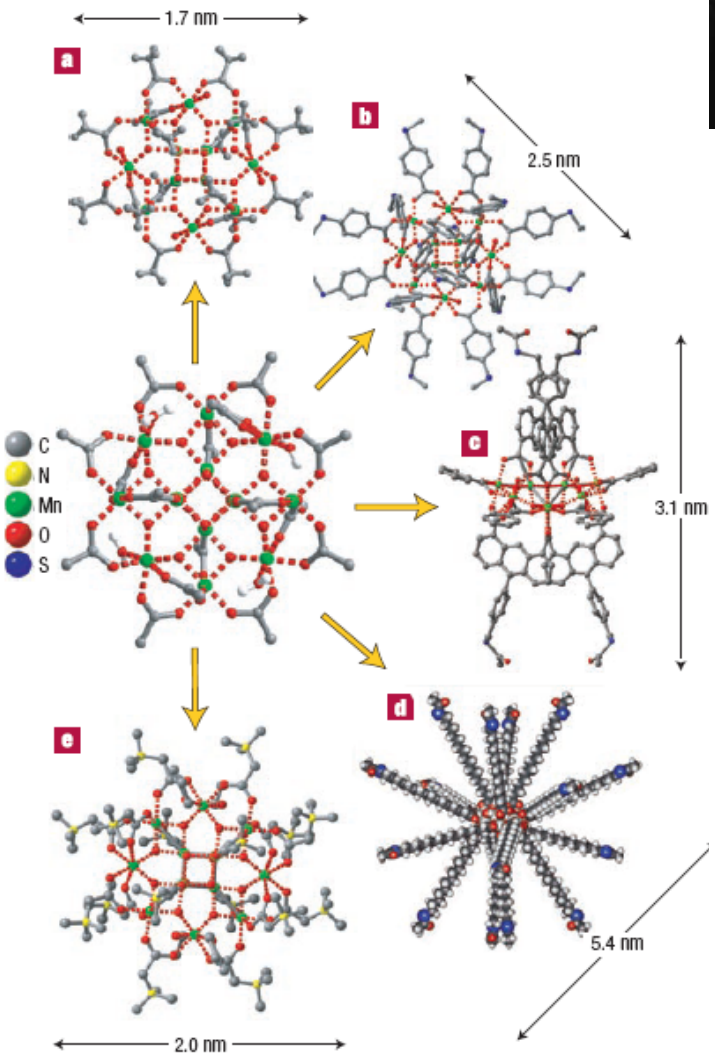

Figure 1 Representative examples of the peripheral functionalization of the outer organic shell of the $[Mn_{12}O_{12}(CH_3COO)_{16}(H_2O)_4]$ SMM (centre). Different functionalizations used to graft the SMM to surfaces are displayed: **a**, $[Mn_{12}O_{12}(C(CH_3)_3COO)_{16}(H_2O)_4]$. **b**, $[Mn_{12}O_{12}(p\text{-}CH_3S\text{-}C_6H_4\text{-}COO)_{16}(H_2O)_4]$. **c**, $[Mn_{12}O_{12}(O_2CC_6H_5)_8$(1,8-dicarboxyl-10-(4-acetylsulphanylmethyl-phenyl)-anthracene-1,8-dicarboxylic acid)$_4(H_2O)_4]$. **d**, $[Mn_{12}O_{12}(CH_3OS(CH_2)_{15}COO)_{16}(H_2O)_4]$. **e**, $[Mn_{12}O_{12}((CH_3)_3NCH_2COO)_{16}(H_2O)_4]^{16+}$. All structures are determined by X-ray crystallography, except **d**, which is a model structure. Solvent molecules have been omitted.

Bogani and Wernsdorfer, Materials Naturals 2007

NOOOOOOOOOOOO !

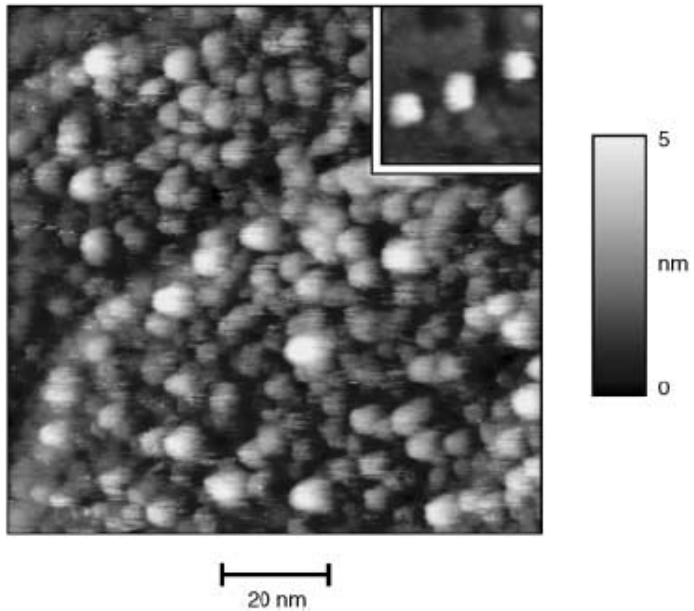

Figure 3. Constant-current STM image of Au-bound Mn_{12} clusters (set-point = 5 pA, bias = 1.3 V, scan size = 100 nm, scan rate = 3 Hz). The inset shows three isolated molecules (setpoint = 10 pA, bias = 0.8 V, scan size = 30 nm, scan rate = 3 Hz).

Cornia et al., Angew. Chem. 2003

SMM deposition in UHV

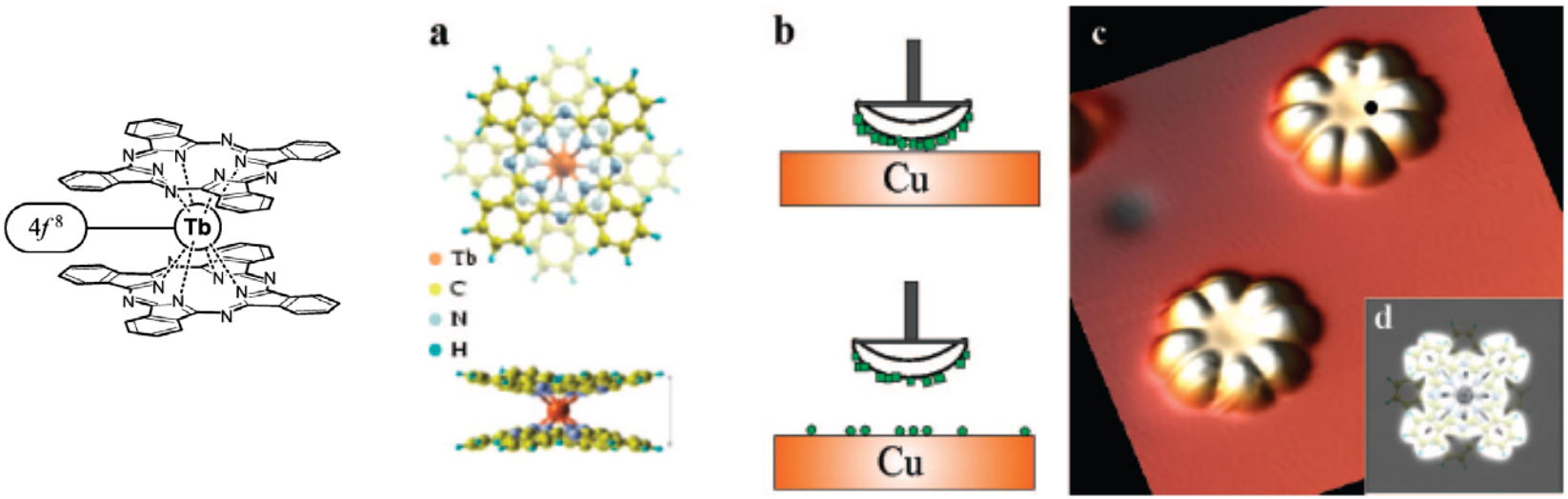

Electronic Structure of Surface-supported Bis(phthalocyaninato) terbium(III) Single Molecular Magnets

Lucia Vitali,*,† Stefano Fabris,‡ Adriano Mosca Conte,‡ Susan Brink,§
Mario Ruben,§ Stefano Baroni,‡ and Klaus Kern†,||

Perhaps, but not yet (ferro)magnetic !

2D spin networks

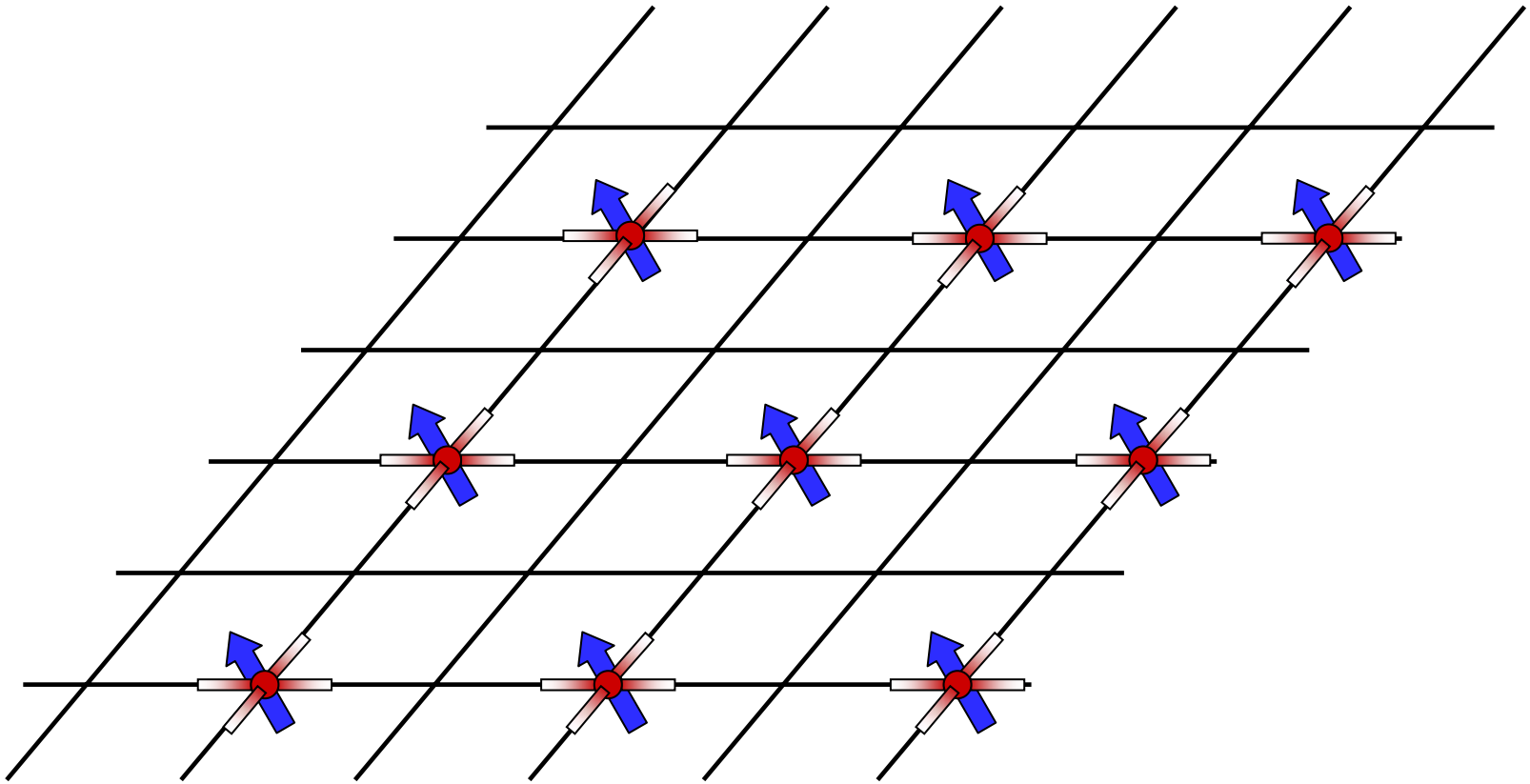

2D self-assembled supramolecular networks

terephthalic acid (TPA)

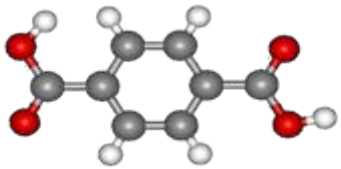

Fe

T_{ads} = 400 K

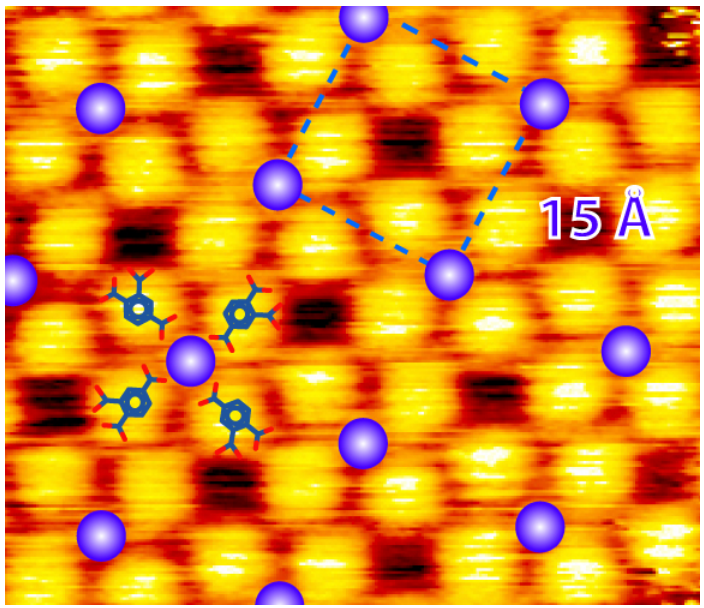

Fe : TPA ≈ 1:4

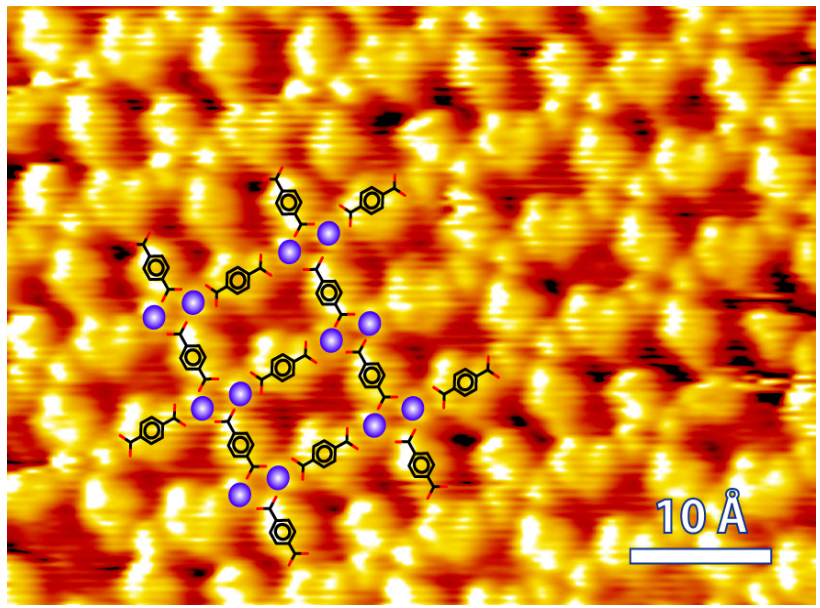

Fe : TPA ≈ 1:1

M. Lingenfelder et al., Chem. Eur. J. **10** (2004) 1913,
P.G. et al. Nat. Mater. **8**, 189 (2009)